Appendix I. Summit tilt calculations and Mogi inflation centers

Modeling of tilt changes

The simplest and most useful way to model the buried inflation and deflation source at Kīlauea is the point Mogi pressure source in an elastic half-space (Mogi, 1958). We state here the theoretical elevation, tilt and total volume relations historically used to model contour maps of elevation changes from leveling surveys, and maps of tilt vectors from tiltmeter arrays. Here d is the horizontal distance from the source center, f is the depth of the source, a is the radius of the source sphere, P is the pressure inside the buried sphere and μ is the rigidity measured in the same units as the pressure. The elevation change when pressure is applied is (Eaton, 1962; Mogi, 1958):

$$\Delta h = \frac{3a^3 P}{4\mu}\left[\frac{f}{(f^2 + d^2)^{3/2}}\right] \qquad (1)$$

We abbreviate the expression $3a^3P/4\mu$ with the letter K (expressed in units of km^3), which is (1) constant for a given episode, (2) determined empirically by the data, and (3) a measure of the strength of the source. The change at the center of inflation (d=0) is $\Delta h_0 = K/f^2$. The integrated volume of the uplift or collapse is $\Delta V = \Delta h_0 2\pi f^2$ (Eaton, 1962). Thus:

$$\Delta V = 2\pi K \qquad (2)$$

and depends only on the strength of the source and not directly on its depth f. This ΔV is the volume of the elastic source but must allow for magma compression before equating to magma volume. The radial tilt change τ around the Mogi source is also a function of distance d and depth f (Eaton, 1962; Jackson and others, 1975):

$$\tau = \frac{K\,3d/f}{f^3(1 + d^2/f^2)^{5/2}} \qquad (3)$$

The maximum tilt τ_m occurs at d=f/2 and is $\tau_m = 0.86K/f^3$. A useful relation is:

$$\frac{\tau}{\tau_m} = 3.5\frac{d/f}{(1 + d^2/f^2)^{5/2}} \qquad (4)$$

The volume change is $\Delta V = 2.32\pi f^3 \tau_m$ (Dzurisin et al, 1984). Thus $\Delta V = 2\pi K$, the same relation as derived from elevation. K (and thus ΔV) can be determined from elevation changes, tilt, or both. It is useful to estimate volume change from a single tiltmeter like Uwēkahuna or Whitney when it is the only record of a single deflation event. Combining equations 2 and 3 yields:

$$\Delta V = \frac{\tau 2\pi\left(1 + d^2 / f^2\right)^{5/2}}{3d / f} = D\tau \qquad (5)$$

The volume factor D can be calculated for each tiltmeter's response to a single source, and may not change much during several inflation/deflation episodes.

The elevation change Δh and tilt τ have different dependencies on the source depth f. The maximum height Δh_0 scales with $\sim f^{-2}$: moving a source deeper rapidly reduces the height of the bulge, but broadens it so that the volume depends only on the strength of the Mogi source. For distances d large compared to the source depth f, $\Delta h \sim Kf/d^3$, for d>>f. The height has a weak dependence on source depth but very rapidly falls off with distance. The maximum tilt τ_m scales with $\sim f^{-3}$, thus tilt diminishes rapidly with increasing source depth, and has a stronger dependence on source depth than the elevation function Δh. For distances d large compared to the source depth f, $\tau \sim 3Kf/d^4$, for d>>f. The tilt on the flanks of the bulge also has a weak dependence on source depth, but falls off very strongly with distance.

At Kīlauea, we estimate the volume change ΔV (essentially the factor K) from a single tilt change τ. The tilt scales linearly with K, once the distance and source depth are known. The tilt has a weak dependence on source depth f, and varies essentially as f to the first power. Tilt has a strong dependence on distance d, however, starting at 0 at d=0, reaching a sharp maximum, and falling off as d to the fourth power. For the d>>f case, $\tau \sim 3Kf/d^4$. A source depth change from 2.5 to 3.5 km produces only a 30% change in tilt, but changing d by 20% changes tilt by 100%. The volume change ΔV does not depend only on the source depth: the source depth (even an approximate one) is needed to calculate the shape of the elevation or tilt curve, but the volume scales with the amplitude of the curve, not its width. It is therefore very important to determine the inflation source location fairly well before scaling ΔV from τ, and to calibrate the ΔV to τ relation for a time period with well-determined source location but not necessarily well-determined source depth. In other words, for a Mogi source of a given strength, changing the lateral position of the source by 1 km can have a much bigger effect on tilt than changing the depth by 1 km.

The location and depth of the Mogi source, or more complicated source approximated with concentric contours, can be determined from a map of level contours or a map of tilt vectors. The level contours are concentric on the source location and their average radii yield a set of distance versus Δh points. A spreadsheet programmed with equation (1) can calculate the elevation profile, and the source depth and intensity K can be determined interactively.

For any two stations, 1 and 2, the depth f of the deformation source can be determined from measuring the tilt magnitude τ and the known distance from each station to the source location and then calculating depth directly from the tilts τ_1 and τ_2, and their source distances d_1 and d_2. Taking the ratio of the tilt equations and solving for f yields

$f^2=(Cd_1^2-d_2^2)/(1-C)$ where $C=(\tau_1 d_2/\tau_2 d_1)^{2/5}$ (6)

A graphic solution may be found for the source location from the average intersection of tilt vectors. The source depth and the constant K (or volume) may then be determined iteratively by fitting tilts (or elevations) and distances with a spreadsheet. Errors of the source determination may be empirically estimated from the fitting or mismatch of elevation contours and the uncircularity of contours. Alternatively, a least-squares solution for the source depth and location can be obtained for measurements from a network of stations using a computer program. This can yield average values for different time periods, but the progression of inflation or deflation centers is best estimated from changes of tilt azimuth over short periods of time.

Examples of fitting a Mogi source

We next examine an example elevation and tilt profile for the 1966–1967 summit inflation (figure I1). This example covers a time when both the leveling and tilt measurements span approximately the same period, and there are adequate measurements to determine the Mogi source. The example also illustrates some problems with using only tilt data. The inflation height contour radii were measured from the October 1967 leveling survey differenced from the January 1966 survey (Fiske and Kinoshita 1969, their figure 4A). The deformation location is near 155º 16.8' west, 19º 23.7' north. The iteratively determined source depth from both elevation and tilt is at 3.3 km. The wet tilt measurements fit the Mogi profile fairly well, except for measurements like Ke'āmoku**,** which typically shows tilt magnitudes much larger than the model fit to other stations, and may have some amplification due to local ground effects. Because there are only 5 independent and un-corrupted tilt stations, and because the tilt curve fit is poorer than the level curve, water tube tilt by itself does not yield a good Mogi solution. The Uwēkahuna long-base tiltmeter is a few hundred meters from the vault housing the short-base tiltmeter, but the two measurements agree fairly well. The calculated volume change from tilt and leveling is 0.056 km^3. The volume factor D estimated for Uwēkahuna from this 1966–1967 episode is about 0.00050 km^3/microradian.

We next plot elevation and tilt profiles for the 1959 inflation and 1960 summit deflation (figure I2). This is not as clean a time period as the 1967 example because the episode includes both inflation and deflation with possible migration of the deformation center, and because the elevation and tilt surveys include overlapping but not identical time periods. The tilt history at Uwēkahuna and Whitney is plotted vs. time in figure A1, showing the amount and timing of pre-eruption inflation and the big January 1960 collapse. The deflation height contour radii (figure I2a) were measured from the May 1960 leveling survey differenced from the January 1958 survey (figure I3; Eaton, unpublished). The deformation location is the same as 1966-67 and is near 155º 16.8' west, 19º 23.7' north. The iteratively determined source depth from elevation contours is at 2.53 +/- 0.05 km, the volume change is 0.070 km^3 (K=0.011 km^3), and the Mogi fit is good over all radii. We estimate a minimum error of 0.05 km based on multiple fit attempts and the scatter of data points within model curves. The lateral error is larger, about 0.2 km based on visual examination of contours and the original leveling points. The Mogi model curves are fit to an average radius of the level contours, and lack of circularity or concentricity of the contours is another source of error. A rigorous statistical inversion of level data and errors is beyond the scope of this paper and is unnecessary for the volcanic conclusions we draw. The tilt solution (addendum figure 3b) uses the water tube tilt changes between January 12, 1959 and July 7, 1960 (HVO tilt file, Asta Miklius, personal communication, 2009). This interval is as close as possible to

the leveling interval, but includes the pre-eruption inflation in 1958–59, the November 1959 eruption, and most of the 1960 deflation. The tilt values (figure I2b), even when the Ke‘āmoku site is excluded, do not define a smooth Mogi curve. The Mogi source at the depth of 2.53 km (determined from the 1/58-5/60 leveling survey) can’t be determined from the noisy and sparse 1/59–7/60 tilt data, and a tilt-based source at 3.0 km depth is equally likely. The volume changes are 0.107 and 0.125 km^3, respectively. Even though the two 1959-60 volumes derived from tilt are very uncertain, they agree within 20–30% of each other, and are larger than the 0.07 km^3 volume determined from leveling because they exclude a year of prior inflation and include two additional months of deflation.

The 1/20/60 – 4/1/60 tilt survey (figure I4), started just after the great deflation had begun, is a large event and is fit as well by a Mogi solution as any Kīlauea an water tube tilt survey can be. We show alternative Mogi solutions at 2.5, 3.0, and 3.5 source depths. We exclude the errant Ke‘āmoku station. The best fit is between the 3.0 km and 3.5 km source depths, where only the first two stations discriminate between those depths. The 2.5 km source depth, found for the 1/58–5/60 leveling survey, which includes the 1/60–4/60 tilt survey and two years of prior inflation, is a poorer fit to the water tube data. This suggests the pre-1960 inflation was centered shallower than 2.5 km, and the 1960 deflation was between 3.0 and 3.5 km.

The tilt results suggest that a well-placed tilt station (like Uwēkahuna or Whitney on the flank of a tilt bulge) can estimate the magnitude of an inflation or deflation to about 20%, once the location and depth of the center is known. The comparisons also suggest that level surveys are much better than tilt surveys to locate inflation centers: even a tilt survey made over the optimum 1/60-4/60 period where the changes are very large can only resolve depths to about a kilometer, but level surveys can resolve Mogi depths to about 0.2 km or better with smaller changes. Water tube tilt was measured more easily by a survey crew over a shorter time period than a level survey, and tilt provides a crude approximation to a level survey. We only use level surveys to estimate inflation/deflation centers (table I1).

The leveling and tilt data suggest the inflation in 1958–1959 was at a shallower 2–2.5 km Mogi center depth than the subsequent 1960 collapse, which was deeper, perhaps between 3.0 and 3.5 km, but this is not well-determined. Figure I2a demonstrates 2.53 km is a good average depth for the 150 microradian inflation and 350 microradian deflation (net 200 microradian deflation) of the whole 1958–60 episode. The 3.0 to 3.5 km source depth of the 1/20/60 – 4/1/60 tilt collapse (figure I4) suggests that the deflation occurred at a depth greater than the average. Thus the inflation (about half of the later deflation) must have been shallower than 2.53 km. We interpret this result to mean that the top of the magma reservoir expands in response to inflation and magma addition, but that deflations, particularly large ones, are centered deeper in the reservoir.

Both source depths and volumes are subject to errors in determination. Note that the source depth f can be fairly well determined by fitting the elevation profile (figure I2a). Estimating the source depth from a tilt profile as equal to twice the distance at which the maximum tilt occurs (figures I1b, I2b) can be more difficult, however: tilt varies widely near its maximum radius and near the source because tilt is very sensitive to non-Mogi irregularities of the source near the surface. Also there is more depth error if only sparse tilt data are available. Both the elevation and tilt curves scale linearly with the volume change ΔV. Thus the volume determination is generally well determined from a profile of height or tilt measurements, and is less sensitive to irregularities in the tilt curve. Choosing a short time period spanning a single but large inflation or deflation episode may yield a better fit from a simple Mogi source. The tilt data and multiple Mogi curves of figure I2b show that even if source depth and location are well known, volume estimates made from a single tilt measurement can easily be in error by about 20–40%, and more if the location is poorly known.

Multiple inflation and deflation centers and reservoir volume relations

We determined a Mogi inflation/deflation source for a large set of published level surveys, and can infer some characteristics of the magma reservoir source. We determined the deformation center locations, depth and volumes from contoured level survey maps using the same methods as in the sample cases above. The Mogi center locations and depths are in appendix figures A2 and I5 along with those of Fiske and Kinoshita (1969). The level profiles with model fits are in figures I6 and I7, and the events and parameters are listed in the table I1.

Most of the Mogi centers strongly cluster in the south caldera, with another smaller cluster in the central caldera. Two centers lie outside the main cluster (10/76–3/77 and 3/77–8/77), one to the south and one to the SW (appendix figure A2). The level surveys for these two centers involve a rift zone contribution and are not a bulls-eye pattern. Both the centers determined in this paper and the Fiske and Kinoshita (1969) centers define the two south and central caldera areas active during this period. The Fiske and Kinoshita centers may scatter a bit more in the east-west direction, but the apparent east-west lineation is not visible in the larger data set and two irregular clusters without an east-west lineation is a better representation of the active area.

We interpret the scatter of different deformation centers as both a shifting locus of magma accumulation and depletion, and the expression of a source that is irregular in shape and definitely not a point source as represented in the Mogi model. The 2 km extent of the sources is larger than the error associated with any one source, and individual error does not contribute much to the extent of sources. Detailed inversions of source shapes are possible using tilt, level and displacement data (eg. Dieterich and Decker, 1975), but we will only generalize that the deforming part of the caldera is an irregular shape about 2 km in diameter in the south caldera.

1924 subsidence

We determined three alternative Mogi models to the 1921–1927 survey which includes the large 1924 eruption and caldera collapse (Wilson, 1935). This was the largest eruption observed geodetically and the maximum deflation was more than twice that in the large January 1960 eruption. The models are for 1, 2 and 3 Mogi sources all centered below Halemaʻumaʻu . The first 1-source model with a deflation center at 1.65 km depth does not fit the level data very well (figure I6a). Adding a shallow deflation source 800 m below Halemaʻumaʻu to a source at a typical 3.8 km depth greatly improves the fit to level contours out to 6 km from the center (figure I6b). Subsidence did not stop at the caldera boundary 6 km from Halemaʻumaʻu, however, and the level line continued through Keaau (39 km from Halemaʻumaʻu) to Hilo. The line to Keaau is almost radial to caldera, but we do not model the dog-leg extension from Keaau to Hilo. A third deflation source at about 30 km depth is required to subside the flank of Kīlauea out to 40 km. We kept the shallow 800m source and moved the 3.8 km source to a depth of 3.5 km to get the best fit (figure I6c). The exact depth and volume of the 30 km source is definitely not well determined because it comes only from fitting the four points along the Volcano highway to Keaau. This is only one radial line and not a concentric set of confirming level curves as would be desired.

There is no geodetic record elsewhere in the past 200 years for a deforming magma source below the base of the crust. And yet Wilson's leveling suggests a source on the order of 30 km distant from the documented sources within the crust beneath Halemaʻumaʻu. We suggest in the text for chapter 3 that the anomalous source is not a deep Mogi source beneath Halemaʻumaʻu, but rather as an eccentric and unlocated source that we postulate as representing the loss of a deep magma system beneath the east rift zone, a loss that extended beyond the documented intrusion near the end of the onshore east rift zone.

Filling and draining of magma reservoirs

The depths of the Mogi inflation/deflation centers illuminate the portions of the magma reservoir that fill between eruptions and drain during different size deflations. Refer to figure I8 showing the distribution of Mogi depths for centers listed in table I1 by the volume change of the event. Most inflation and deflation centers are between 3 and 4 km deep, and this is the most active part of the reservoir. All but one of the centers between 2.0 and 2.9 km are small inflation centers. This means the top of the active reservoir is just above 2 km depth. The exception to the small inflation in the upper reservoir rule is the 1/58–5/60 period, which includes two years of inflation followed by a larger deflation, with a net average depth of 2.5 km. Of course the upper reservoir can participate in other events, which also include volume changes in other parts of the reservoir and have deeper average Mogi centers. We exclude the 10/76–3/77 event as a special case: it is south of the caldera and is separated from the other centers laterally and is much deeper at 6.0 km. This center occurred during the recovery after the *M*7.2 Kalapana earthquake in which the south flank moved laterally south up to 6 m, and probably represents filling of the deeper voids in the Koae fault zone created by the earthquake as well as filling the shallow magma reservoir.

The largest volume reservoir events (>0.06 km^3) are different in distribution from the smaller events (figure I8). On average, the smaller events (<0.06 km^3) tend to inflate at a shallow center between 2.0 and 3.6 km, but small rapid deflation events are between 3.0 and 3.8 km. The four largest deflationary points include collapses from the 1924 eruption, the Nov. 1975 earthquake, and the Jan–Feb 1960 eruption (which is included in two survey periods). These four deflationary points have a linear trend where the larger the volume change, the deeper the deflation center. This means the draining must tap deeper parts of the reservoir to gain more magma volume change, and the deflation center moves downward as more of the deeper reservoir is tapped. The depths of different sized inflation and deflation sources means the reservoir tends to add magma at its top (like filling a pail) and to subtract magma lower down (like opening a valve on the side of a pail).

The linear relation of volume change of the largest deflations to the Mogi depth, and the observation that all volume changes lie below this line (figure I8), suggest that there is a geometric relation between the change of liquid magma and the total reservoir volume. The line defined by the four large deflations is $\Delta V = 0.089(f-1.75)$ where ΔV is the magma volume change in km^3, and f is the depth of the Mogi center. The intercept of this linear relation (1.75 km) and the shallowest observed Mogi depth (2.0 km) suggest that we assume the top of the reservoir is at 1.75 km. Let us also assume for modeling purposes that the active reservoir is a sphere centered at depth f. The deepening of this active reservoir with magma volume change also means the size of the active reservoir increases with depth. If we model the top of the reservoir at a depth of 1.75 km, its radius is f-1.75 and its volume V is $4\pi/3\ (f-1.75)^3$. The volume fraction of inflating/deflating magma is $\Delta V/V$, which in our model depends on f. For Mogi depths of 2.5, 3.0 and 3.5, the liquid to total volume fractions are 3.7%, 1.3% and 0.68%. Wright and Klein (AGU 2010) noted that erupted/intruded magma batches in mid-20^{th} century Kīlauea eruptions had volumes of about 0.2 km^3, which for a reservoir diameter of 3 km, yields a liquid fraction of 1.4%, the same as our middle value. The hypothesized relation between liquid fraction and depth means that larger, deeper deflations have smaller liquid magma fractions by volume, and small shallow events have more liquid. Note that the observed volume changes in figure I8 are all below this maximum line because many volume changes occur within a spherical volume that does not reach the top of the reservoir at 1.75 km. Thus the top of the reservoir is mostly liquid and the bottom is mostly solid, which agrees with the lower density of magma compared to rock. Of course this reasoning is based on a simplified point model and is qualitative in nature.

Whitney tilt volume calculations

In an effort to determine magma center volume changes from a single tiltmeter, we examine the simpler period of January 20 to April 1, 1960, during which Kīlauea summit underwent a massive deflation associated with the East rift eruption of 1/13–2/19/1960. Unfortunately there is no level survey for this interval, but the deflation is included in a longer interval from 1/58 to 5/60 for which a level survey exists (table I1, event 1). We can use this 1960 deflation as an example of estimating source depth from two tiltmeters and volume change from a single tiltmeter. The tilts are 275 and 199 microradians and the source distances are 3.2 and 3.8 km for the short-base water tubes at Uwēkahuna and Whitney, respectively. Equation (6) thus yields a source depth of 3.0 km. Comparison of measured portable water-tube tilts and a calculated Mogi source at 3.0 km depth (figure I4) confirm the 3.0 km depth and a volume of

0.107 km^3 as a good fit to the tilt data, excluding Ke‘āmoku as an amplified site. Note that (figure I5) the location of the two tiltmeters on the flank of the tilt bulge does not give a good resolution of the source depth but does measure the height of the tilt curve. The tradeoff between volume and source depth of the three curves of figure I4 means that for variation of +/- 0.5 km from its average source depth of 3.0 km, the magma volumes vary by +/- 20%. The volume error will be more than these interdependence variances. These tiltmeters gives similar volume estimates. From appendix table A2, the ratio of Whitney to Uwēkahuna tilt for a depth of 3 km is 1.38. We apply this ratio to the Dvorak factor for Uwēkahuna of 0.00045 km^3/micro-radian to yield 0.00062 km^3/micro-radian for the conversion of Whitney tilt magnitude to volume. We use this factor for the volume calculations during periods before 1960 when the only measurements were tilt made at the Whitney vault.

Given the good fit of a Mogi source to the water-tube tilts of the 1960 deflation, what volume changes do the continuous tiltmeters at Uwēkahuna and Whitney imply? We can both calculate theoretical volume factors from the 3.0 km source using equation (5), and determine empirical factors from the 0.107 km^3 source volume determined from all 7 tiltmeters. Equation (5) applied to Uwēkahuna yields a theoretical volume factor of D_{UT}=0.00035 km^3/microradian. The empirical volume factor using 275 microradians of deflation and a 0.107 km^3 source determined by the Mogi curve fit imply that D_{UE}=0.00039 km^3/microradian for Uwēkahuna. The empirical value is probably a better one to use because it uses volumes calculated by an array of tiltmeters and includes a tiltmeter site correction. The 0.107 km^3 source volume was determined by fitting a curve to an array of 7 tiltmeters, not just the tiltmeter whose volume factor we are determining. Increasing the theoretical volume factors calculated from equation (5) by 10% should empirically correct other sources measured at Uwēkahuna. Note that the Uwēkahuna short-base tilt in the 1966–67 inflation (figure I1b) similarly requires a positive 20% correction to match the Mogi source determined by the tiltmeter array. The empirical volume factor is similar to the summit volume factor value of 0.00045 km^3/microradian used by Dvorak and Okamura (1985) and Dvorak and Dzurisin (1993). Each tiltmeter will have its own volume factor D because it depends on the distance and depth to the source.

The theoretical volume factor for the Whitney tiltmeter and the 1960 deflation source is D_{WT}=0.00049 km^3/microradian, which is somewhat larger than the Uwēkahuna factor because Whitney is farther from the source. The empirical factor for Whitney is D_{WE}=0.00054 km^3/microradian. The theoretical volume factors for Whitney also require a 10% correction. Using equation (5) and typical deformation centers (table I1), we can calculate a table of tiltmeter volume factors for various Mogi locations and depths, and apply the 10% empirical correction (see table I2). The Dvorak factor for Uwēkahuna that we use (0.00045 km^3/micro-radian) corresponds to a source depth of ~ 3.8 km in appendix table A1. The tilt factor applied to the Pu‘u ‘Ō‘o -Kupaianaha (PK) eruption gave an eruption efficiency of 1.01 for deflation azimuths near Fiske-Kinoshita center 1. The dike volume estimated for the dike associated with episode 1 of the PK eruption is higher by a factor of 1.5 than the volume estimated by the tilt deflation (Hall Wallace and Delaney, 1995). If this volume is used in the summation of text table 7.8, the eruption efficiency is close to or slightly less than 1.

References

Bevens, D., Takahashi, T.J., and Wright, T.L., eds., 1988, The early serial publications of the Hawai‘ian Volcano Observatory, 3 v.: Hawai‘i National Park, Hawai‘i Natural History Association, v. 1, 565 p.; v. 2, 1273 p.; v. 3, 1224 p.

Dvorak, J.J., and Dzurisin, D., 1993, Variations in magma supply rate at Kīlauea Volcano, Hawai‘i: Journal of Geophysical Research, v. 98, no. B12, p. 22, 225–22, 268.

Eaton, J.P., 1959, A portable water-tube tiltmeter: Bulletin of the Seismological Society of America, v. 49, no. 4, p. 301–316.

Eaton, J.P., 1962, Crustal structure and volcanism in Hawai‘i, in Crust of the Pacific Basin: American Geophysical Union Geophysical Monograph 6, p. 13–29. [National Academy of Science, National Research Council Publication 1035]

Fiske, R.S., and Kinoshita, W.T., 1969, Inflation of Kīlauea volcano prior to its l967–l968 eruption: Science, v. 165, p. 341–349.

Fiske, R.S., Simkin, T., and Nielsen, E.A., eds., 1987, The Volcano Letter: Washington, D.C., Smithsonian Institution Press, 539 p. [Compiled and reprinted; originally published, 1925–1955, by the Hawai‘ian Volcano Observatory]

Hall Wallace, M., and Delaney, P.T., 1995, Deformation of Kīlauea Volcano during 1982 and 1983: a transition period: Journal of Geophysical Research, v. 100, no. B5, p. 8201–8219.

Jackson, D.B., Swanson, D.A., Koyanagi, R.Y., and Wright, T.L., 1975, The August and October 1968 east rift eruptions of Kīlauea Volcano, Hawai‘i: U.S. Geological Survey Professional Paper 890, 33 p.

Mogi, K., 1958, Relations between the eruptions of various volcanoes and the deformations of the ground surfaces around them: Bulletin of the Earthquake Research Institute, v. 36, p. 111–123.

Wright, T.L., and Klein, F.W., 2006, Deep magma transport at Kīlauea volcano, Hawai‘i, in Edwards, B.R., and Russell, J.K., eds., Mantle to Magma—Lithospheric and Volcanic Processes in Western North America: Lithos, 87, 1–2, 50–79.

Appendix table I1: Inflation/deflation centers derived from leveling contour maps.

seq.	start	end	Inf /def	lat d	lat m	lon d	lon m	F km	K(km^3)	Offset (m)	dV (km^3)	reference	geologic events	comments
0a	1921	1927	def	19	24.8	155	17.2	1.65	0.0091	-1.1	0.0571	Wilson 1935	1924 Halem. eruption	Two depth sources are required to fit levelling curve. (a) is single source
0b	ditto	ditto	ditto		ditto		ditto	0.8, 3.8	0.0016, 0.03	-0.6	0.010, 0.1884	ditto	ditto	(b) is two sources at 0.8 and 3.8 km depth which fits better & is good geologically
0c	ditto	ditto	ditto		ditto		ditto	0.8, 3.5, 30	0.0016, 0.024, 0.73	0.09	0.010, 0.15, 4.6	ditto	ditto	(c) is three sources which fits the caldera very well and the Volcano-Keaau level line toward Hilo. A spherical Mogi source at 30 km gives too large a volume, but deep or tectonic movement is required.
1	Jan-58	May-60	def	19	24.68	155	16.60	2.53	0.0112	0	0.0703	Eaton unpub	major ERZ eruption	Includes eruption deflations in 11/59 and 1-2/60 & prior inflations. +/-0.05 depth error
	1/20/1960	4/1/1960	Def		ditto		ditto	3.0-3.5	-	-	0.107-0.132	HVO water tube tilt files	ditto	Water tube tilt result, less precise than leveling, last part of above period.
2	7/1/1960	4/1/1963	inf	19	23.91	155	16.84	3.2	0.012	0.07	0.0754	Moore & Krivoy 1964 fig 4	summit & ERZ erupns.	NE transect
3	3/9/1965	7/15/1965	inf	19	24.84	155	16.53	3.3	0.001	0.023	0.0063	Wright et al 1968 fig 6		Map only shows contours, not benchmarks. Inflation after 3/5/65 eruption.
4	Jan-66	Jul-66	inf	19	24.26	155	16.64	2.95	0.001	0.012	0.0063	Fiske & Kinoshita 1969 fig 4b		Fiske & Kinoshita center 1.
5	Jul-66	Sep-66	inf	19	24.92	155	16.60	3.5	0.0013	0.025	0.0082	Fiske & Kinoshita 1969 fig 4c		Possible additional small shallow source. Fiske & Kinoshita center 2.
6	Jan-66	Oct-67	inf	19	23.86	155	16.74	3.3	0.009	0.095	0.0565	Fiske & Kinoshita 1969 fig 4a		
FK3	Oct 1966	Jan 1967		19	23.76	155	16.44							Fiske & Kinoshita center 3.
7	1/12/1967	2/27/1967	inf	19	23.70	155	17.20	2.9	0.0012	0.025	0.0075	Dieterich & Decker 1975 fig 11		North transcect. Fiske & Kinoshita center 4.
FK5	Feb 1967	Feb 1967		19	23.76	155	17.64							Fiske & Kinoshita center 5.
FK6	Feb 1967	May 1967		19	23.52	155	16.86							Fiske & Kinoshita center 6.
FK7	May 1967	June 1967		19	23.52	155	16.68							Fiske & Kinoshita center 7.
FK8	June 1967	July 1967		19	23.82	155	17.10							Fiske & Kinoshita center 8.
FK9	July 1967	Sept 1967		19	23.82	155	16.14							Fiske & Kinoshita center 9.
8	Sep-67	10/31/1967	inf	19	23.60	155	16.89	3.4	0.00145	0.017	0.0091	Kinoshita et al, Phys Volc fig 11		Map only shows contours, not benchmarks. Transect to N. 2x error in scale on map. Inflation before 1967-68 summit eruption. Fiske & Kinoshita center 10.
9	10/31/1967	11/10/1967	def	19	23.46	155	16.73	3.8	0.001	0.023	0.0063	Kinoshita & Koyanagi 1969 fig	11/5/67 caldera erupt	Average of NW & NE transects; "-1.5" cm contour approximate.
9a	11/10/1967	7/15/1968	Inf /def									Kinoshita & Koyanagi 1969 fig		Not Mogi source: Halemaumau deflates, Keanakakoi inflates.
10	7/15/1968	8/28/1968	def	19	23.86	155	16.61	3.0	0.0025	0.025	0.0157	Jackson et al 1975 fig 13	8/68 ERZ eruption	Contours elongate to NW-SE, N transect.
11	8/28/1968	10/10/1968	def	19	23.78	155	16.66	3.7	0.0028	0.026	0.0176	Jackson et al 1975 fig 32	10/68 ERZ eruption	Contours elongate to NS, innermost contour offset to south, NW transect.

12	7/15/1968	10/10/1968	def	19	23.94	155	16.64	3.2	0.0045	0.055	0.0283	Jackson et al 1975 fig 35	two ERZ eruptions	Includes two previous periods.
13	2/5/1969	3/5/1969	def	19	24.18	155	16.92	3.7	0.0018	0.012	0.0113	Swanson et al 1976 fig 20	2/69 ERZ eruption	N-S kidney shaped contours.
14	2/9/1970	5/20/1970	inf	19	23.47	155	16.63	2.5	0.0012	0.012	0.0075	Duffield et al 1976 fig 7		Shallow deflation source 2 km NE of inflation center; elongate source.
15	6/8/1971	8/25/1971	inf	19	24.24	155	16.55	2.3	0.0012	0	0.0075	Duffield et al 1982 fig 4	8/14/71 caldera erupt	Kidney shaped contours; average of E and W transects; possible deep ~30 km source may improve curve fit.
16	8/25/1971	9/30/1971	inf	19	24.13	155	17.46	2.0	0.0019	0.02	0.0119*	Duffield et al 1982 fig 9	9/24/71 SWR eruption	Intrusion made an inflation signal, not deflation. Elongated contours follow SW rift; volume thus underestimed; NW transect from uprift end of source.
17	9/30/1971	1/20/1972	inf	19	23.98	155	16.98	3.6	0.0042	0.04	0.0264	Duffield et al 1982 fig 10b		Includes deflation after 9/24/71 SWR eruption plus subsequent inflation.
18	11/30/1971	1/20/1972	inf	19	23.76	155	16.80	3.5	0.0023	0.025	0.0144	Tilling et al 1987 fig 16.38		Subset of previous period, primarily with inflation and no deflation.
19	6/12/1972	12/13/1972	def	19	23.87	155	17.40	4.6	0.017	0.15	0.1068	Ryan et al subsidence mech fig 15		average of NW and SE transects
20	12/4/1972	5/12/1973	def	19	23.82	155	16.64	3.7	0.00154	0.022	0.0097	Ryan et al subsidence mech fig 18	5/5/73 ERZ eruption	East rift has a non-Mogi dike intrusion deformation, but caldera has Mogi src.
21	11/13/1973	4/5/1974	inf	19	24.68	155	16.65	2.6	0.00048	0.05	0.0030	Lockwood et al 1999 fig 17a		Complex pattern in S & E caldera; inner contour not fit by model and may require a very shallow sourcel; SW transect
22	4/4/1974	7/31/1974	inf	19	24.40	155	16.42	3.0	0.0019	0.004	0.0119	Lockwood et al 1999 fig 17b		SSE transect, contours elongate to NE.
23	7/26/1974	10/1/1974	inf	19	24.16	155	17.24	2.9	0.0021	0.014	0.0132	Lockwood et al 1999 fig 17c		East transect; contours elongate to NE.
24	9/30/1974	1/13/1975	def	19	24.10	155	16.94	3.0	0.007	0.06	0.0440	Lockwood et al 1999 fig 17d	SWR eruption	Average of NW & NE transects; inner contour poorly fit.
25	Jan-75	Sep-75	inf	19	23.68	155	16.74	3.3	0.0064	0.05	0.0402	Lipman et al 1985 fig. 17b		
26	Sep-75	Jan-76	def	19	23.72*	155	16.84*	3.4	0.022	0.4	0.1382*	Lipman et al 1985 fig. 17c	M7.2 earthquake	Elongate dike-like bulge along SWR and diminished central bulge relative to Mogi model. Mogi volume is thus overestimated for summit, but total volume including SW extension may be underestimated by Mogi model.
27	Jan-76	Sep-76	def	19	23.74	155	16.71	3.5	0.0041	0.107	0.0257	Lipman et al 1985 fig. 17d		Post earthquake deflation; ERZ deflation from intrusions.
28	Oct-76	Mar-77	inf	19	23.19	155	16.42	6.0	0.0049	0.03	0.0308	Lipman et al 1985 fig. 17e		Southerly, deep deflation center; one ERZ intrusion.
29	Mar-77	Aug-77	def	19	22.85*	155	18.30*	3.1	0.00068	0.01	0.0043*	Lipman et al 1985 fig. 17f		Mogi fit to west end of elongate depression across south caldera with small bump in middle. Actual source is maybe 2x larger and more irregular than Mogi.
30	8/25/1977	9/23/1977	def	19	23.92	155	16.74	3.5	0.0059	0.05	0.0371	Lipman et al 1985 fig. 17g	ERZ eruption	West transect. Excellent Mogi fit.
31	Dec-83	Nov-91	def	19	23.45	155	16.94	3.7	0.00118	-0.003	0.0074	Delaney et al 1993 fig 5	ERZ eruption	Steady deflation sustained Puu Oo eruption. Total from 8 yr average.
32	1996	2002	Def	19	23.40	155	16.43	3.2	0.004	-0.025	0.025	Cervelli and Miklius 2003 fig 5	ERZ eruption	Steady deflation sustained Puu Oo eruption. Total from 6 yr average.

(*) Irregular source shape, Mogi elevation contours not a good fit, but source depth may be OK.
Contours roughly circular unless noted otherwise. Mogi a good fit unless noted with *. Transect through contours taken to give "average" radii to the NW or N unless noted otherwise. Zero contour assumed to be arbitrary and chosen at an outer benchmark within deformation zone, thus the offset factor adjusts the data to a baseline to fit the Mogi curve.

Appendix table I2. Long-base water-tube tilt vectors 1960-1965

Cycle	Begin	End	Lon.	Lat.	Mag.	Az.	Comment	Reference
1960	12/28-31/1959	9/22-24/1960	155.278	19.404			[i]TM; U; K[ii]; SS[iii] A[iv]; deflation	
	12/29/1959	9/24/1960			72.82	122.69	Match water-tube[v]	
	1/13/1960	2/21/1960					**Eruption—lower east rift zone**	
	1/18/1960	7/24/1960			77.03	124.01	1960 deflation[vi]	
1960-1961	9/16/–24/1960	7/21–25/1961	155.279	19.399			TM; U; K; SS; A; inflation	
	9/19/1960	7/23/1961			54.22	306.14	Match water-tube	
	7/24/1960	9/21/1961			67.98	305.69	1960-1961 inflation	
	9/21/1961	9/25/1961		19.399			**Eruption—middle east rift zone**	
	7/21–25/1961	10/6–11/1961	155.280				TM; U; K; SS; A; deflation	
	7/22/1961	10/7/1961			25.00	135.87	Match water-tube	
	9/21/1961	9/30/1961			35.73	135.82	1961 deflation	
1961-1962	10/6–11/1961	10/26–11/1/1962	155.2815	19.399			TM; U; K; SS; A; inflation	1
	10/7/1962	10/29/1962			21.19	302.75	Match water-tube	2
	9/30/1961	12/6/1962			25.13	301.36	1961-1962 inflation	13; 14
	12/7/1962	12/9–12/1962					**Eruption—upper east rift zone**	2
	10/26–11/1/1962	12/10–12/1962	155.282	19.399			TM; U; K; SS; A; deflation	
		12/12/1962					Match water-tube	
					1.98	147.26	1962 deflation	
	12/6/1962				4.85	133.47		
1962-1963	12/10–12/1962	3/18–21/1963	155.280	19.400			TM; U; K; SS; A; inflation	3
	12/12/1962	3/20/1963			7.05	325.64	Match water-tube	
	5/8/1963	5/12/1963					**Intrusion-Koae fault zone**	
	5/8/1963	5/12/1963	[vii]		7.22	126.27	deflation	
	3/18–21/1963	5/10–14/1963					TM; U; K; SS; A; mixed	4
	3/20/1963	5/13/1963			5.64	91.21	Match water-tube	
	7/2/1963	7/4/1963					**Intrusion-Koae fault zone**	
	6/27/1963	7/2/1963			4.91	119.64	deflation	
	5/10–14/1963	7/3–6/1963					TM; U; K; SS; A[viii]; mixed	5
	5/13/1963	7/5/1963			2.55	332.24	Match water-tube	
	7/3–6/1963	8/5–12/1963	155.283	19.397			TM; U; K; SS; A; inflation[ix]	6
	7/5/1963	8/7/1963			2.67	290.85	Match water-tube	
	8/21/1963	8/23/1963					**Eruption—upper east rift zone**	
	8/20/1963	8/22/1963			2.37	112.07	deflation	

Appendix table I2 cont.

Cycle	Begin	End	Lon.	Lat.	Mag.	Az.	Comment	Reference
	8/5–12/1963	8/22-23/1963	nd	nd			TM; A; south of FK centers	7
	8/22/1963	10/4/1963			5.61	282.67	inflation	
	10/5/1963	10/6/1963					**Eruption—middle east rift zone**	
	10/4/1963	10/10/1963			16.62	124.36	deflation	
	8/5–12/1963	10/7-11/1963	155.278	19.395			TM; U; K; SS; A[x] deflation	8
	8/7/1963	10/9/1963			12.46	131.52	Match water-tube--deflation	
1963-1965	10/7-11/1963	1/17-19/1965	155.280	19.400			TM; U; K; SS; A—inflation	9
	10/9/1963	1/18/1965			17.84	300.41	Match water-tube—inflation	
	10/10/1963	3/5/1965			21.46	302.13	Inflation—entire period	
	1/17-19/1965	3/6-8/1965	155.277	19.399			TM; U; K; SS; A--deflation	10
	1/18/1965	3/7/1965			14.40	126.44	Match water-tube--deflation	
	3/5/1965	3/15/1965					**Eruption—middle east rift zone**	
	3/5/1965	3/9/1965			18.10	128.36	Syn-eruption deflation	
	3/6-8/1965	8/30-9/7/1965	155.275	19.406			TM; U; K; SS; A--inflation	11
	3/9/1965	9/5/1965			5.84	287.10	Match water-tube--inflation	
	3/9/1965	12/23/1965			11.21	281.58	Inflation—entire period	
	12/25/1965	12/25/1965					**Eruption—upper east rift zone**	
	12/23/1965	12/28/1965			9.85	98.33	deflation[xi]	
	8/30-9/7/1965	12/27-30/1965	15.275	19.399			TM; U; K; SS; A--deflation	12
	9/5/1965	12/28/1965			4.43	101.61	Match water-tube--deflation	

References

1(Koyanagi and others, 1963; Krivoy and others, 1963; Krivoy and others, 1964); 2 (Krivoy and others, 1964); 3 (Koyanagi and others, 1964); 4 (Krivoy and others, 1965); 5 (Koyanagi and others, 1964); 6 (Koyanagi and others, 1964); 7 (Koyanagi and others, 1964); 8 (Okamura and others, 1964?); 9 (Kinoshita and others, 1965?; Koyanagi and others, 1965; Koyanagi and others, 1965; Okamura and others, 1965; Okamura and others, 1966); 10 (Okamura and others, 1966); 11 (Koyanagi and others, 1966; Powers and others, 1966); 12 (Koyanagi and others, 1969); 13 (Okamura and others, 1963); 14 (Okamura and others, 1964)

[i] Long-base water-tube tilt stations in use: Tree Molds; Uwekauna; Keaumoku; Sand Spit; Ahua (figure 18). One additional station (Kalihipaa) lies to the south of the network on the map. Magnitudes are small and azimuths from this station are not used.
[ii] The Keaumoku station vector is consistently ~10 degrees more southerly than the intersection of the other vectors
[iii] Sand Spit lies very close to the centers of inflation/deflation and its azimuth determines the direction to the center
[iv] The Ahua station vector is consistently ~10 degrees more westerly than the intersection of the other vectors
[v] Results from the daily readings in Uwekahuna vault measured over the same time interval as the long-base network
[vi] Results from the daily readings in Uwekahuna vault measured over the entire period of inflation or deflation
[vii] Inconsistent tilt intersection. Ahua (southernmost station) shows deflation toward Koae fault zone—other stations mixed
[viii] Ahua shows inflation toward Koae—still recording recovery from Koae intrusions
[ix] Ahua shows deflation toward the Koae-still showing effects of Koae intrusions
[x] Anomalous deflation toward east rift zone associated with Koae deformation and intrusion
[xi] Ahua shows deflation toward Koae; Uwekahuna, Tree Molds and Sand spit show deflation toward east rift zone

Figure I1. Comparison of leveling contour radii (*A*) and water-tube tilt surveys (*B*) around Kīlauea Caldera for the nearly identical time periods of the two survey types (March 1966–November 1967 for tilt, January 1966–October 1967 for leveling). Leveling data from Fiske and Kinoshita (1969); water-tube tilt data from the files of the Hawaiian Volcano Obsrvatory. The same Mogi model is compared to both data sets—source depth of 3.3 km; source volume of 0.056 km^3. The Mogi fit was to the level data, which is much better at determining the location and depth of the Mogi center. The tilt data confirms that a Mogi source fit can only approximate the tilt data. Tilt data, particularly from a short-base tiltmeters in a vault, has the advantage of frequency of measurement. The tilt at the Uwēkahuna Vault closely matches the Mogi model and thus is a good measure of source volume, assuming the source is about 3 km distant. For locations of the long-base water-tube tiltmeters, see figure I5.

Figure I2. Comparison of leveling contour radii (*A*) and water-tube tilt surveys (*B*) around Kīlauea Caldera for the overlapping but nonidentical time period including the major 1960 collapse. The source depth of 2.53 km is well determined for the January 1958–May 1960 leveling interval. A depth error of about +/-0.05 km is a minimum error because it only considers misfit of the average radii data points to the Mogi model and not other error sources (see text). The same source depth (with an adjustment for a slightly larger volume change) adequately fits the tilt data for the shorter January 1959–July 1960 period. A deeper Mogi source at 3.0 km (blue curve in *B*) improves the tilt fit for the shorter time interval, however. For locations of the long-base water-tube tiltmeters, see figure I5.

Figure I3. Elevation changes in the Kīlauea summit region, from 1958 to July 1960. Contour interval in feet. The primary zone of subsidence is centered on Halemaʻumaʻu Crater. A secondary zone of subsidence is defined near Makaopuhi Crater on Kīlauea's east rift zone. This is an area of secondary magma storage and intrusion that has also been active during subsequent eruption cycles (Jackson and others, 1975, figure 32; Moore and Krivoy, 1964, figure 4; Swanson and others, 1976b, figure 4). Finally, the changes along the Hilina Pali road, traversing the Koaʻe Fault Zone between the east rift and south flank, show seaward tilting in the Koaʻe,

and relative uplift of the south flank across the Kalanaokuaiki Pali. This uplift is consistent with movement of magma from the upper parts of Kīlauea's east rift zone combined with seaward movement of Kīlauea's south flank. This is also in agreement with the south-southeast azimuths of Whitney tilt vectors shown in text figure 4.3 during this period. (Contour map produced by the Topographic Division of the U.S. Geological Survey at the request of Jerry Eaton. Based on unpublished data of Jerry Eaton).

Figure I4. Tilt values from the water-tube tilt array for the major caldera collapse from 20 January to 1 April 1960. Also plotted are Mogi model curves for three different source depths. The large size of the tilt values relative to background noise mean this is the best data in the Kīlauea water-tube tilt record to constrain a Mogi source, yet there is still uncertainty with regard to the source depth. A depth of 3.0–3.5 km fits better than the shallow 2.53-km depth for the longer period that includes both inflation and deflation (figure I2). Fortunately, the Uwēkahuna Vault is well placed to record the the source amplitude (for volume calculations) and is relatively insentive to source depth because the model curves intersect near the 3-km distance of Uwēkahuna for this source location. For locations of the long-base water-tube tiltmeters, see figure I5.

Figure I5. Location of inflation-deflation centers. Using Mogi models: Tiltmeter locations are shown as green triangles, and locations of inflation and deflation centers as red circles. The green stars are centers from the mid 1960s identified by Fiske and Kinoshita (1969). The blue symbols are locations of the long-base water-tube tilt network. Red x's are geographic features. The blue symbols (keyed to depth) in appendix A figure A2 (not shown here) are inflation and deflation centers determined in this study and listed in appendix table I1. Using long-base water-tube network: Tilt vectors are tabulated and plotted in Hawaiian Volcano Observatory seismic summaries. As the tilt vectors do not intersect in a point, the location is estimated by eye from the various plots. The Sand Spit and Outlet stations lie very close to the centers of inflation/deflation located south-southeast of Halema'uma'u. The locations plotted use The Sand Spit tilt vector to place the deformation epicenter, even though intersections from other pairs of stations, for example Tree Molds and Uwēkahuna, may lie on the opposite side of Sand Spit from that indicated by the vector at Sand Spit. The

centers of inflation and deflation all lie within the Fiske-Kinoshita array within an area of 1 km^2 marked by black oval and are approximately equidistant from Uwēkahuna. Time periods covered by inflation (+) and deflation (-) centers are labeled as follows:

Centers of inflation			Centers of deflation		
Label	Begin date	End date	Label	Begin date	End date
i1	9/23/1960	7/23/1961	d1	12/30/1959	9/23/1960
i2	10/9/1961	10/30/1962	d2	10/30/1961	12/11/1962
i3	12/11/1962	3/20/1963	d3	7/23/1961	10/9/1961
i4	7/5/1963	8/10/1963	d4	8/10/1963	10/9/1963
i5	10/9/1963	1/18/1965	d5	1/18/1965	3/7/1965
i6	3/7/1965	9/3/1965	d6	9/3/1965	12/29/1965

Figure I6. Elevation profiles vs. radius from the Mogi inflation/deflation center, determined for the 1924 subsidence measured between 1921 and 1927, assuming a single source (*A*), two sources (*B*) or three surces (*C*). See table I1 for the Mogi sources.

Figure I7. Elevation profiles vs. radius from the Mogi inflation/deflation center, determined for the set of 32 survey time periods after 1924 that are listed in table I1. The elevation vs. distance data are for the average radius from all published elevation contour maps the authors could locate in the literature. The iteratively determined Mogi fits are also plotted. The sub-figure numbers (01 to 32) are keyed to survey numbers in table I1.

Figure I8. Mogi volume changes vs. Mogi source depths for the set of time periods listed in table I1. The inflation center depths (squares), which are almost exclusively in the range from 2.0 to 3.5 km, average less than the deflation depths (diamonds), which are concentrated in the range of 3.0 to 3.8 km. This means the reservoir tends to expand near its top, but deflate from lower down near 3–4 km. The four largest volume deflations nearly form a line which is an empirical limit to the size of the maximum deflation, with

larger deflations limited to Mogi centers lower in the reservoir. This linear relation of volume to depth, when combined with the assumption that the top of the reservoir is at about 1.75 km depth, predicts that the percentage of the active fraction of magma increases with shallower depths. Thus the top of the reservoir is mostly liquid and the bottom is mostly solid.

Appendix fig I1. Leveling data 1/66-10/67 (Fiske and Kinoshita 1969)
Water tube tilt data 3/16/66 - 11/7/67 (HVO files)
Mogi model for both: 3.3 km source depth, 0.056 km^3 source volume

A

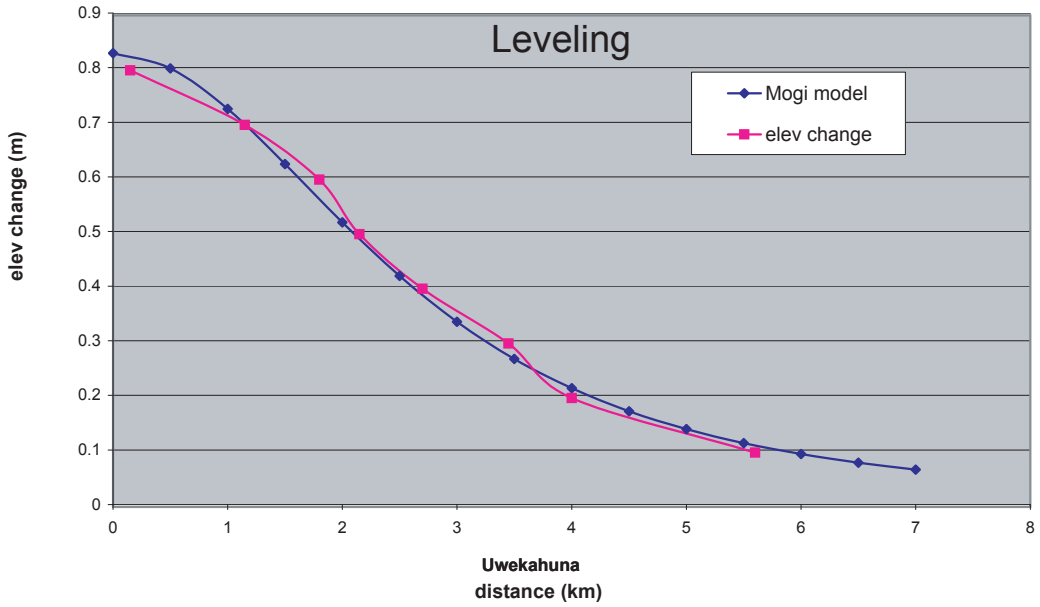

B

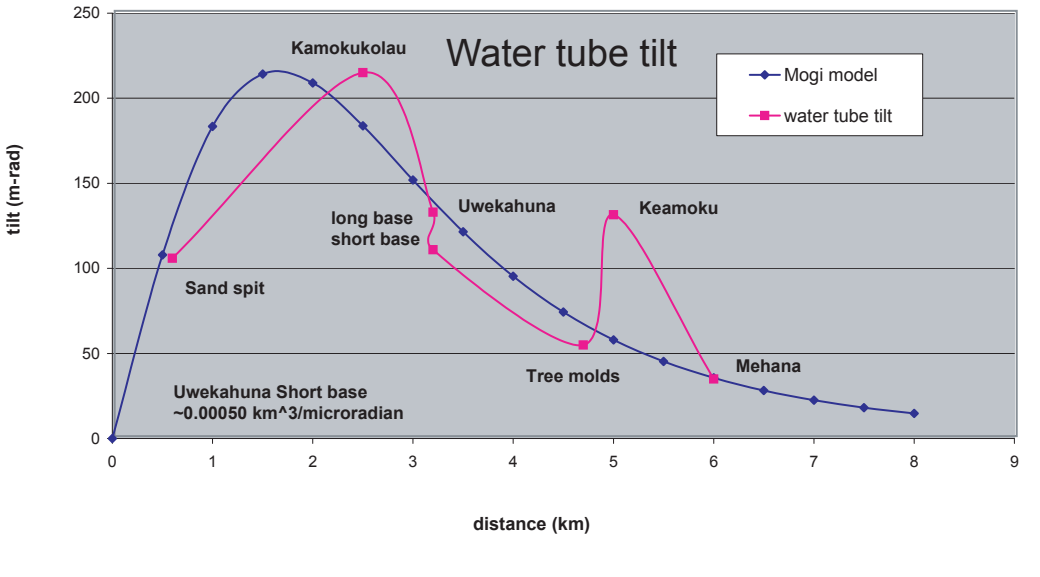

Appendix fig I2.

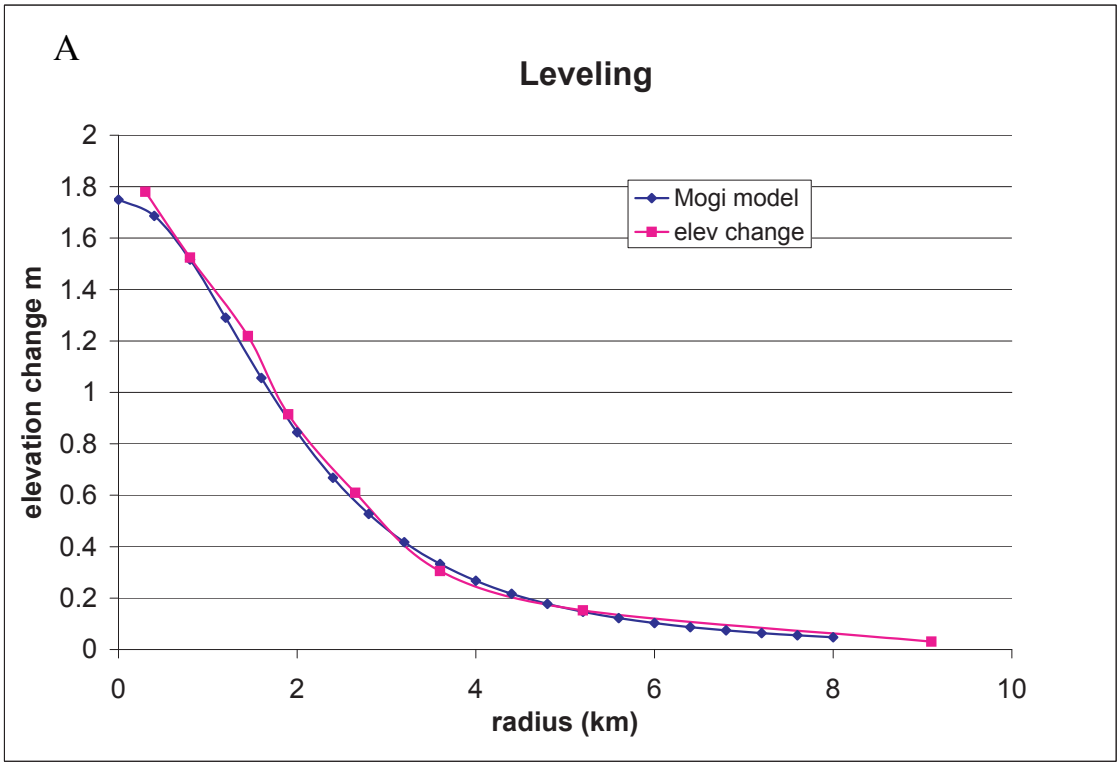

a. 1/58-5/60 inflation & collapse. 2.53 km deep source, deflation volume 0.07 km^3.

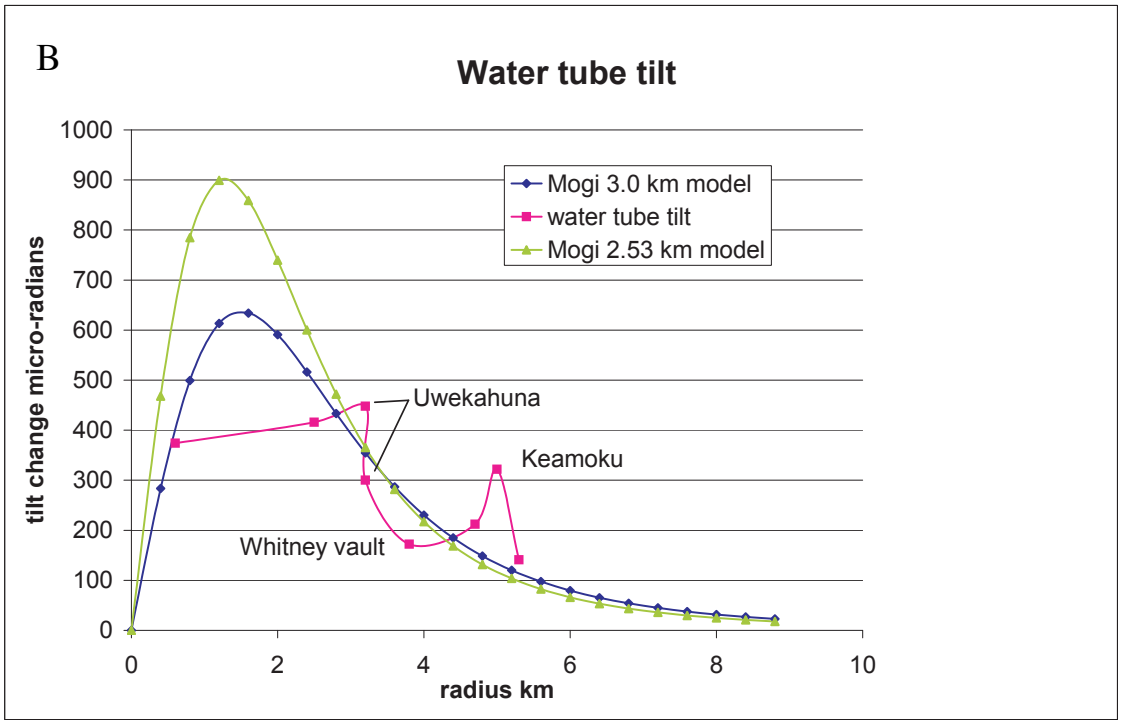

b. 1/12/59-7/7/60 inflation & collapse. 3.0 km deep source, deflation volume 0.125 km^3. Alternative 2.53 km deep source, deflation volume 0.107 km^3

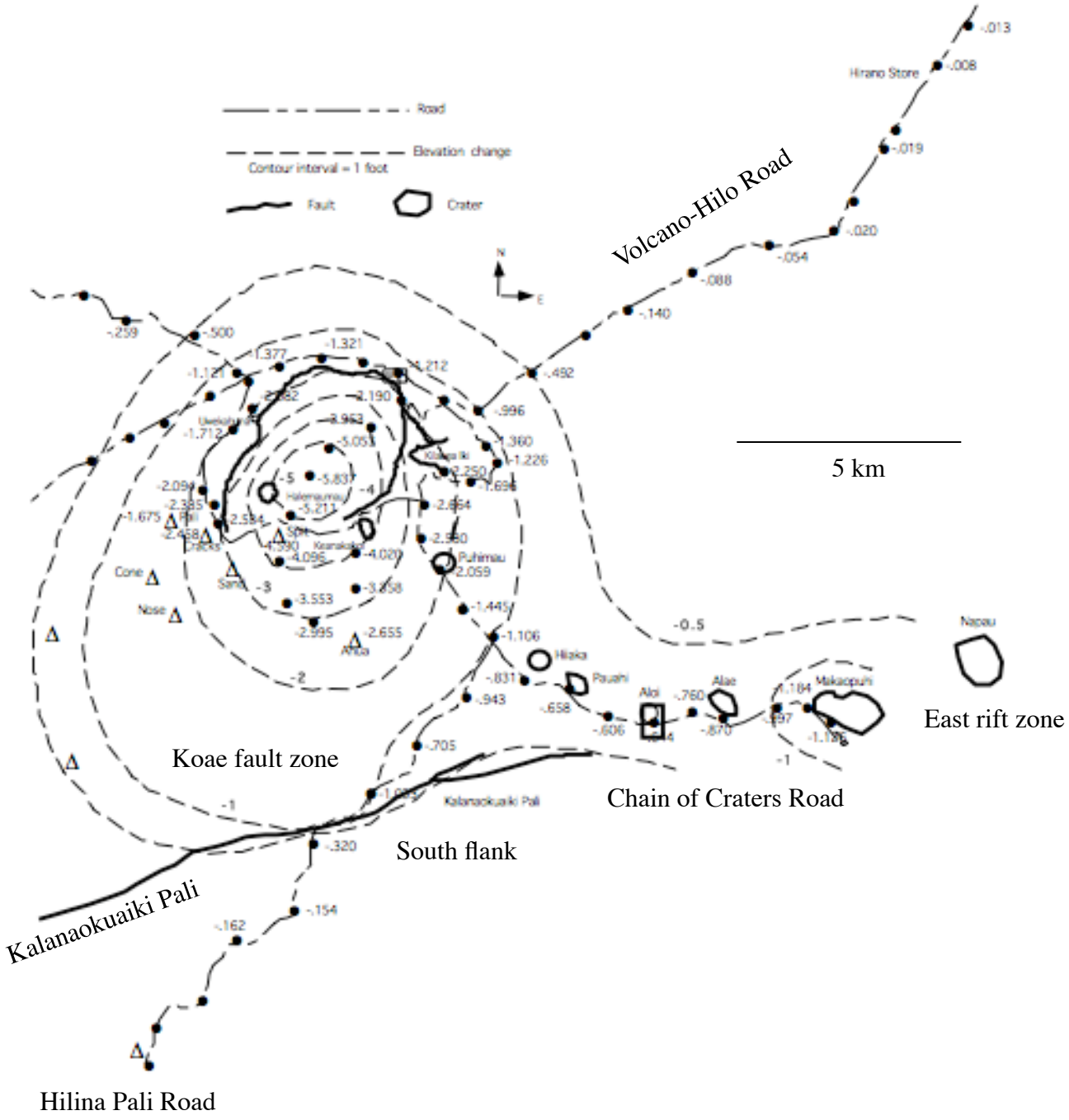

Figure I3. Elevation changes, 1958-July 1960 [Run by the Topographic Division of the U.S. Geological Survey at the request of Jerry Eaton; unpublished data courtesy of Jerry Eaton]

Appendix fig I4. 1/20/60 - 4/1/60 collapse, water tube tilt

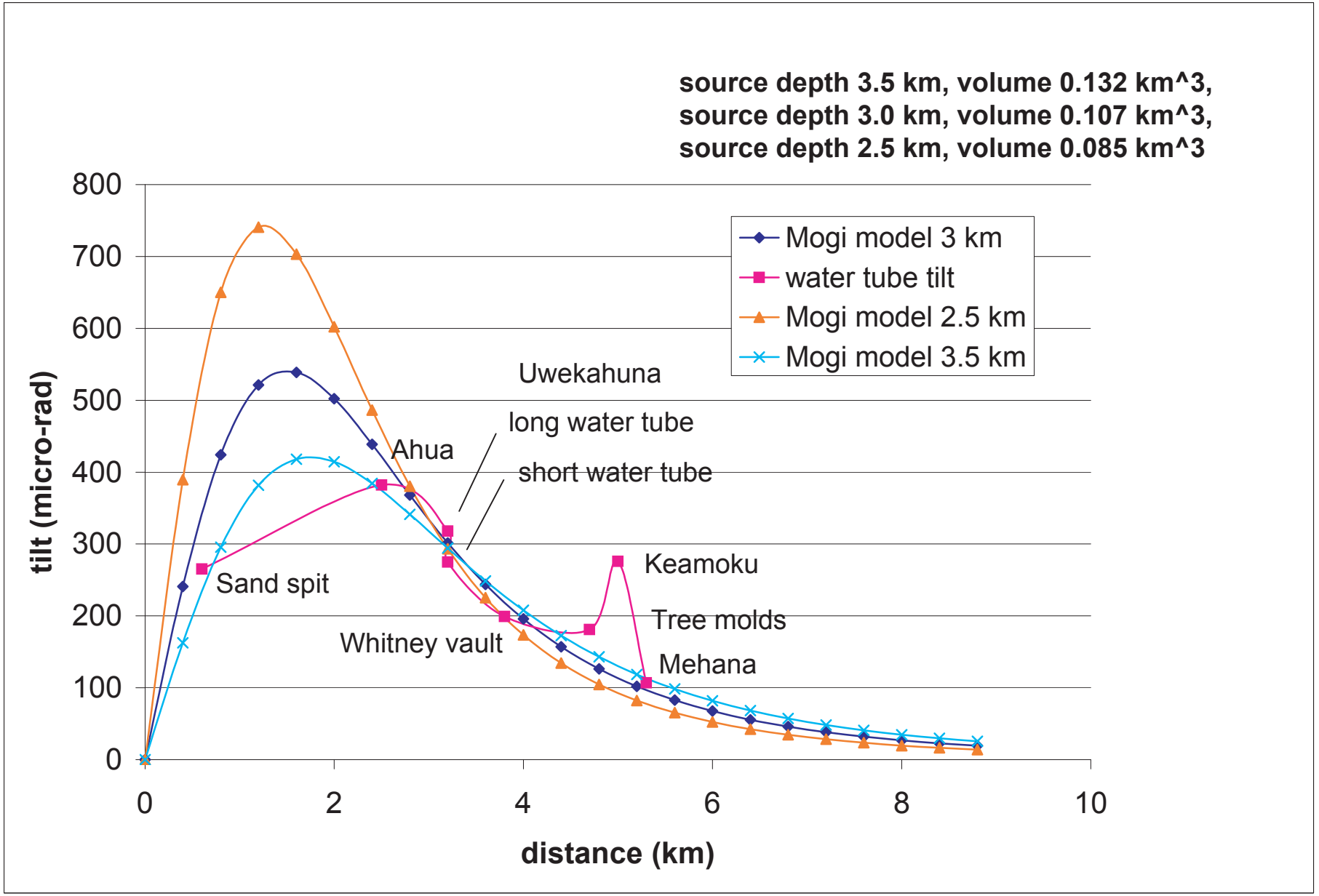

Appendix I. Figure I5 Inflation/deflation centers determine from the long-base water tube network

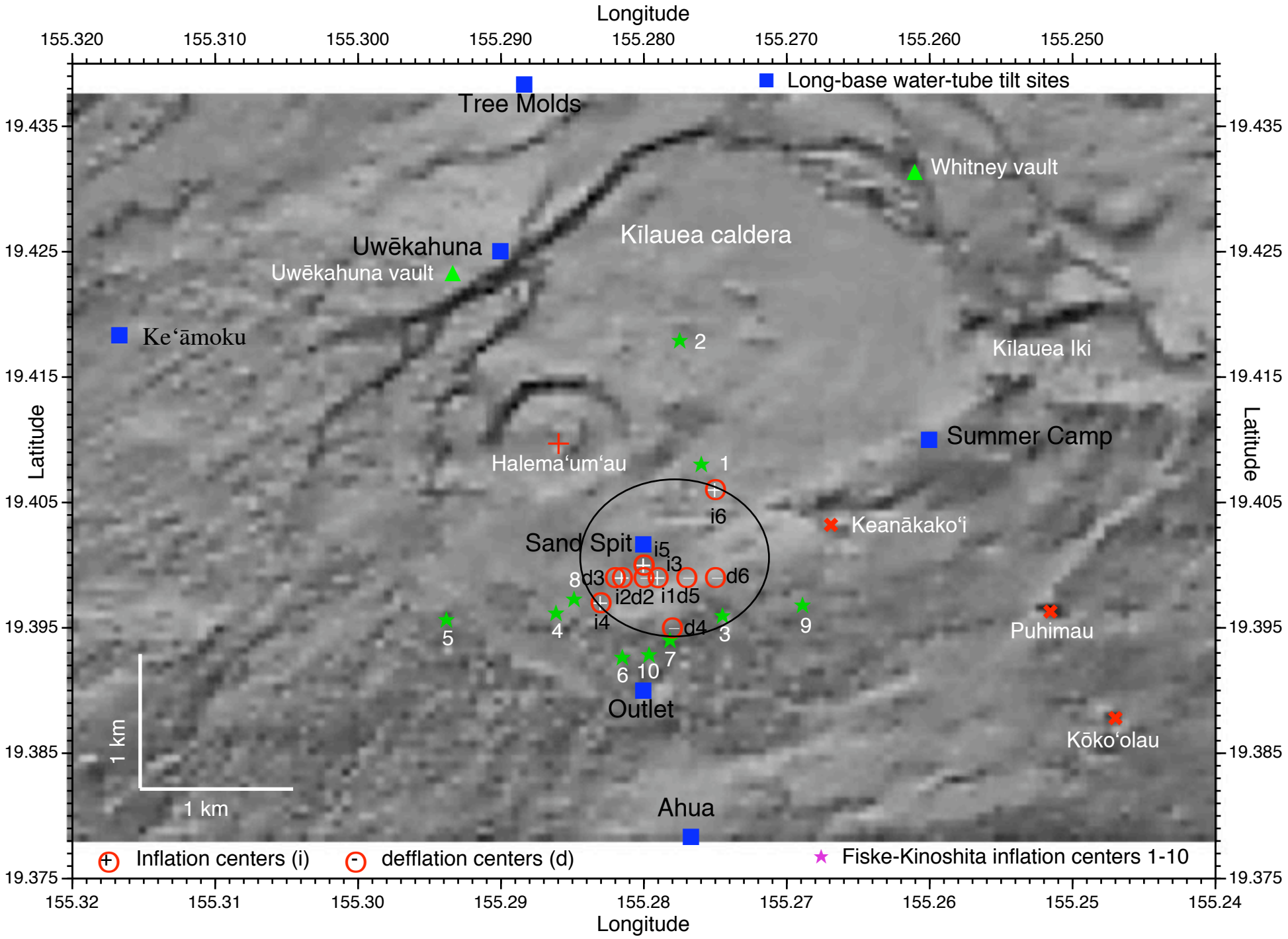

Appendix fig. I6. Mogi model fits to contoured levelling data. See addendum table I1 for Mogi source data.

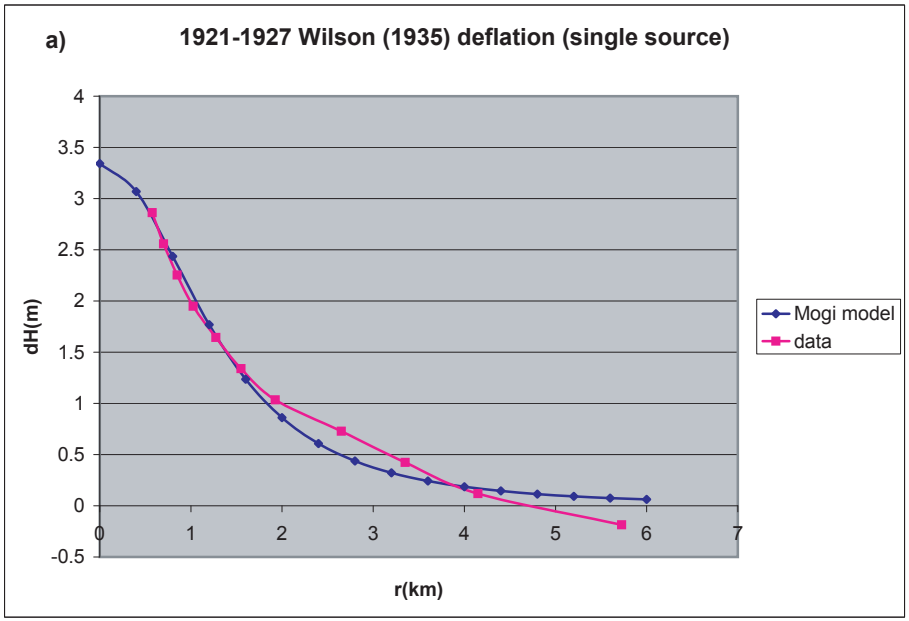

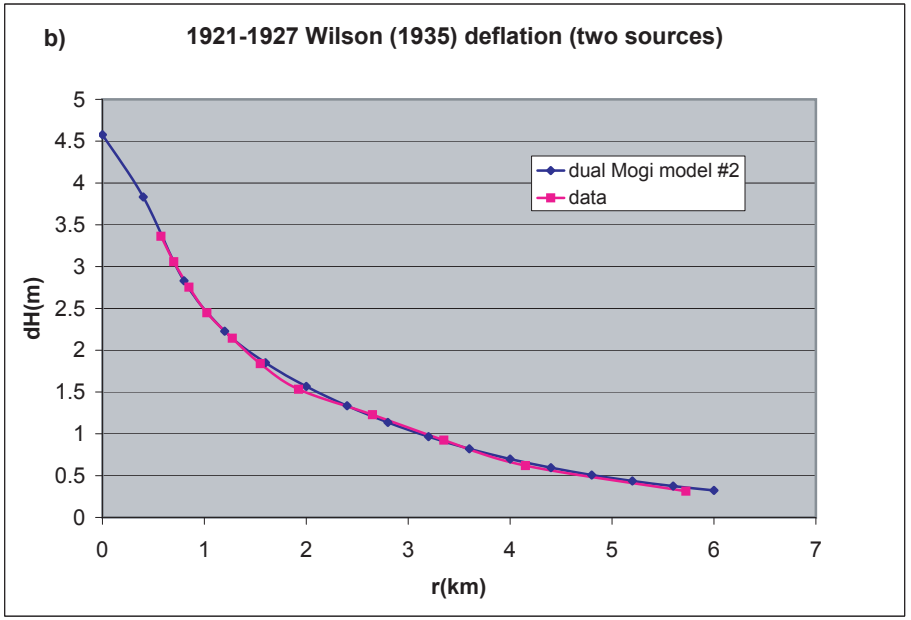

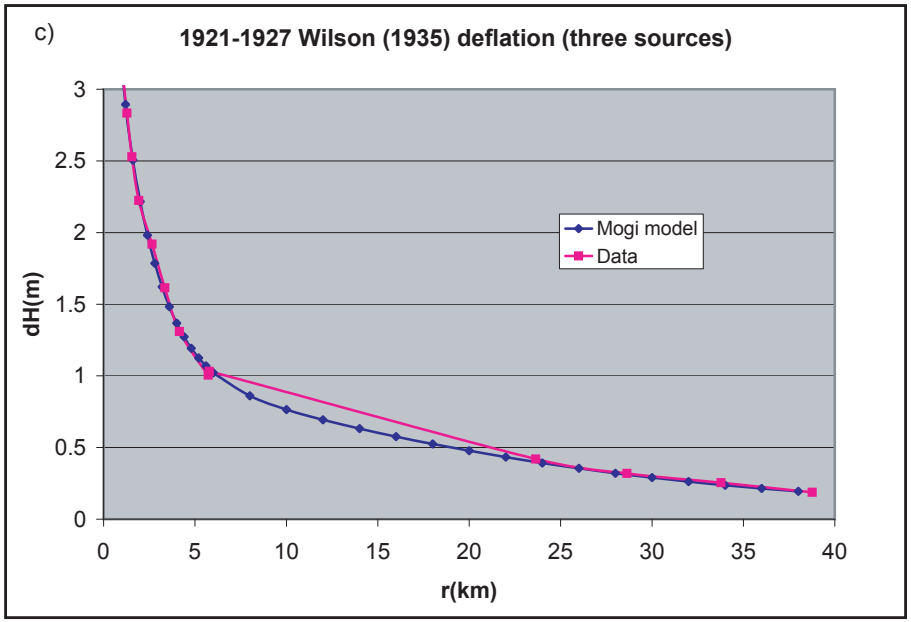

Appendix fig. I7.01-04. Mogi model fits to contoured levelling data. See table I1 for Mogi source data.

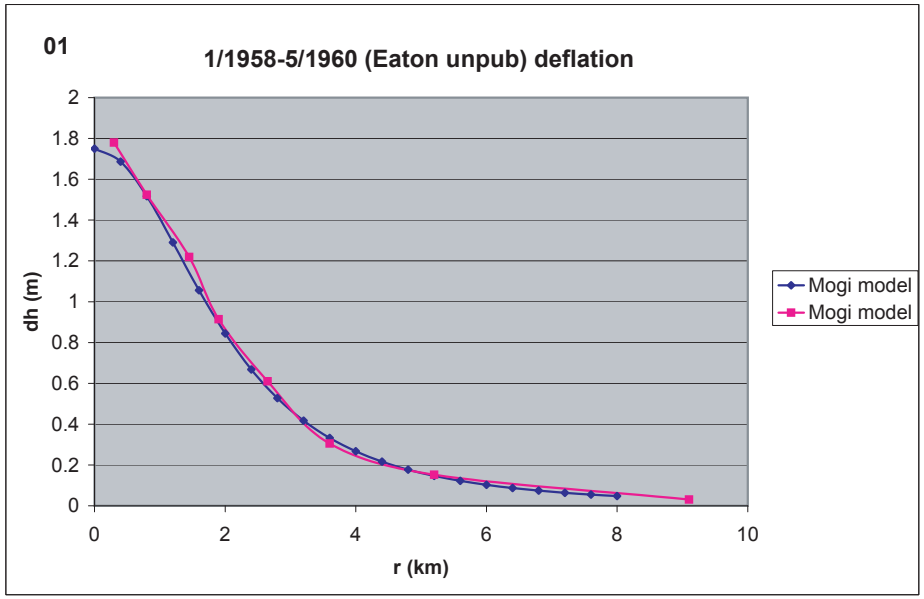

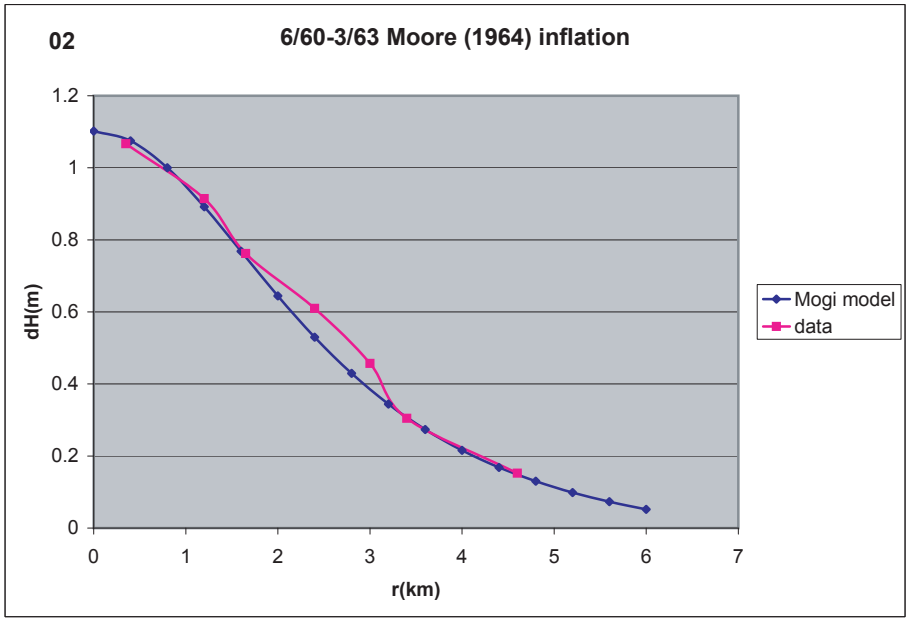

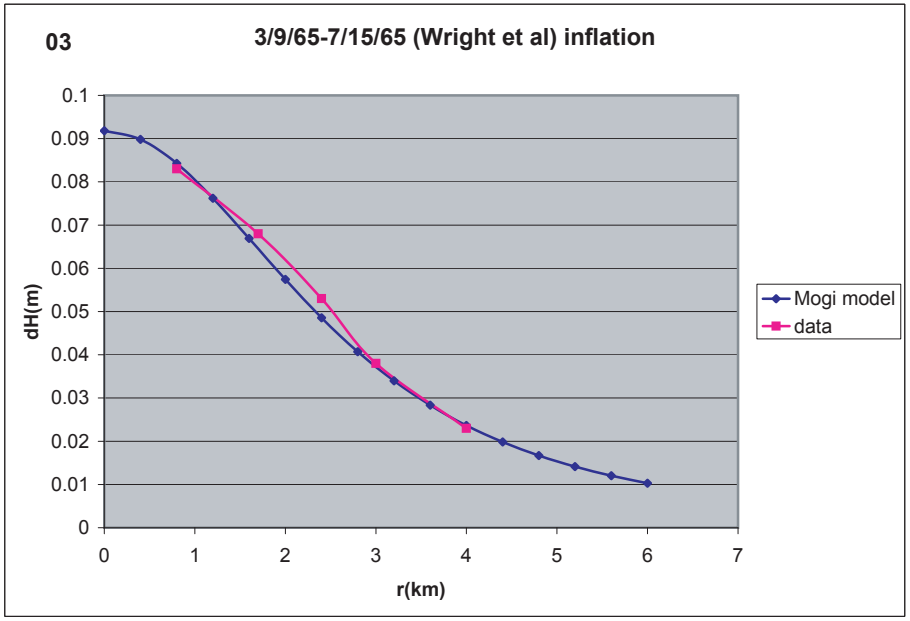

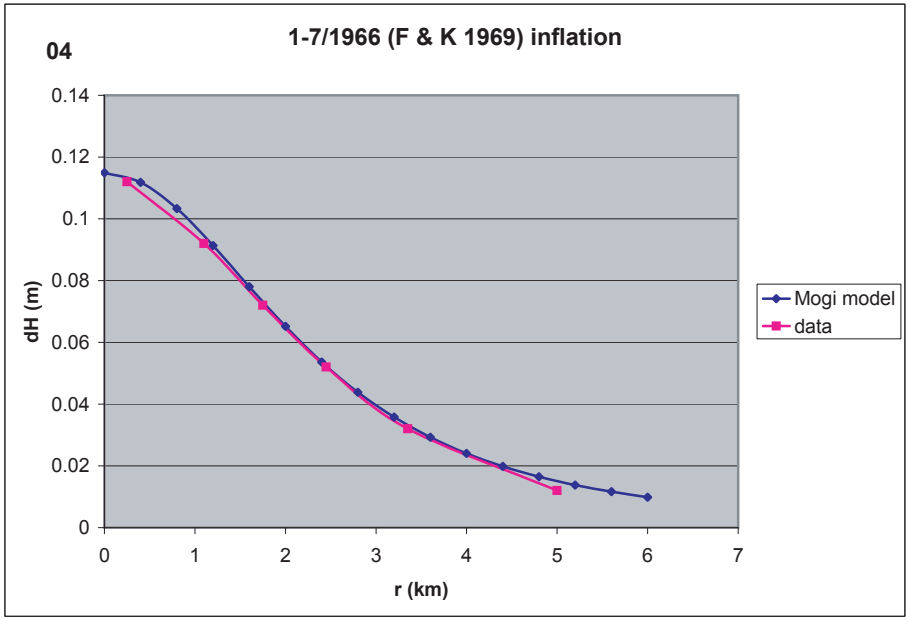

Appendix fig. I7.05-08. Mogi model fits to contoured levelling data. See table I1 for Mogi source data.

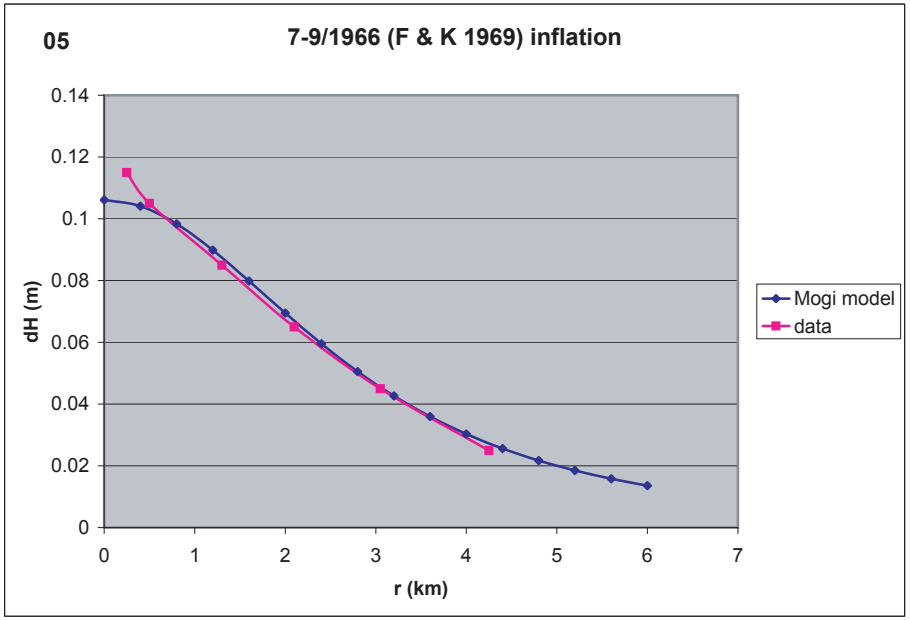

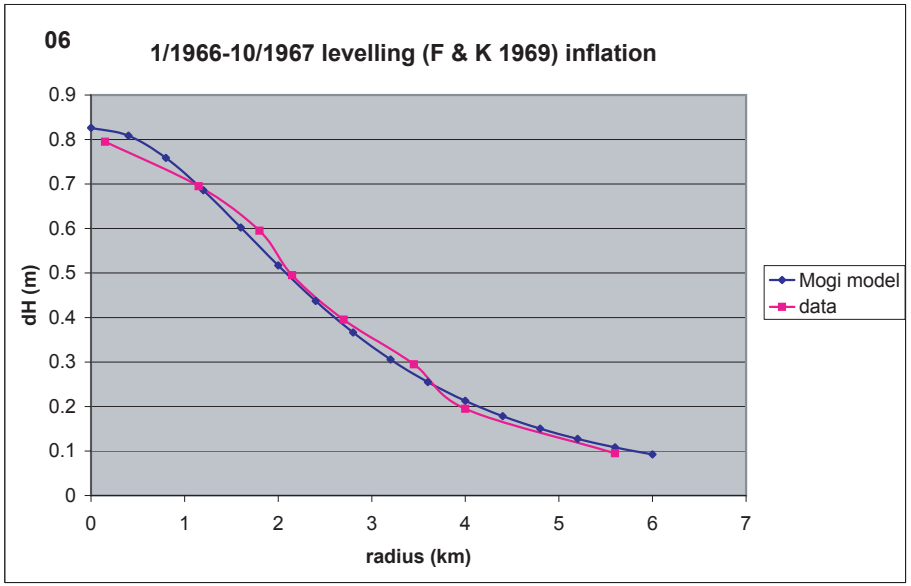

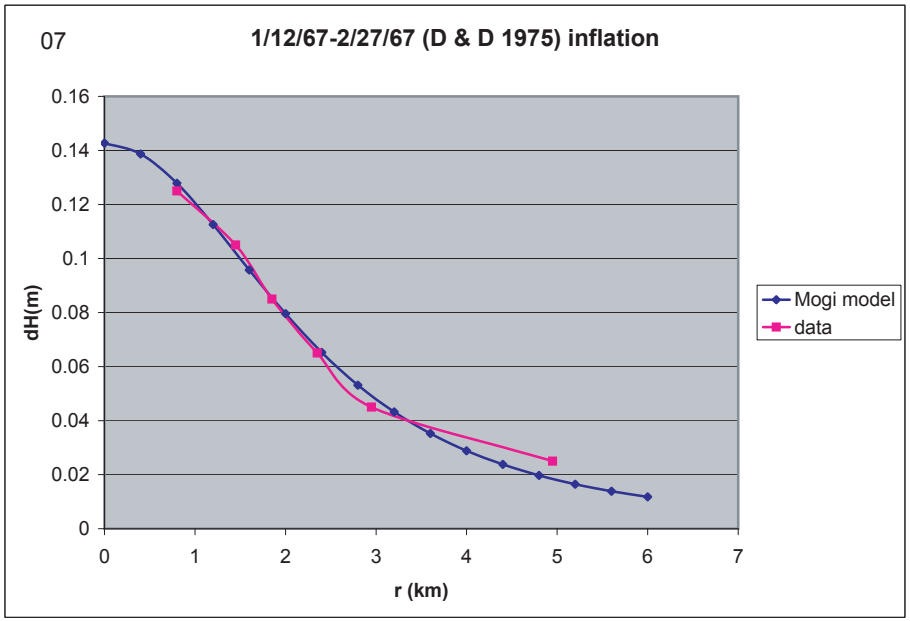

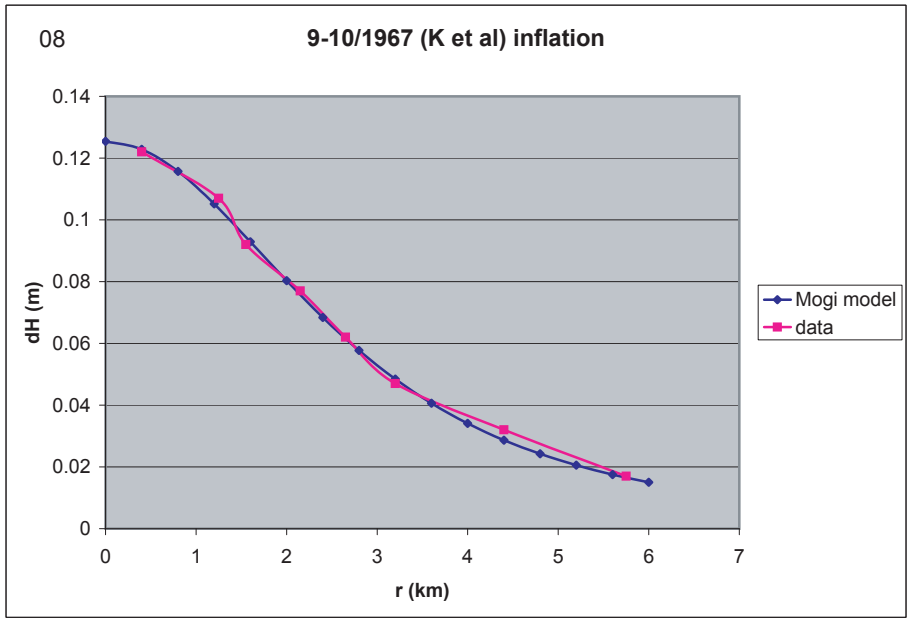

Appendix fig. I7.09-12. Mogi model fits to contoured levelling data. See table I1 for Mogi source data.

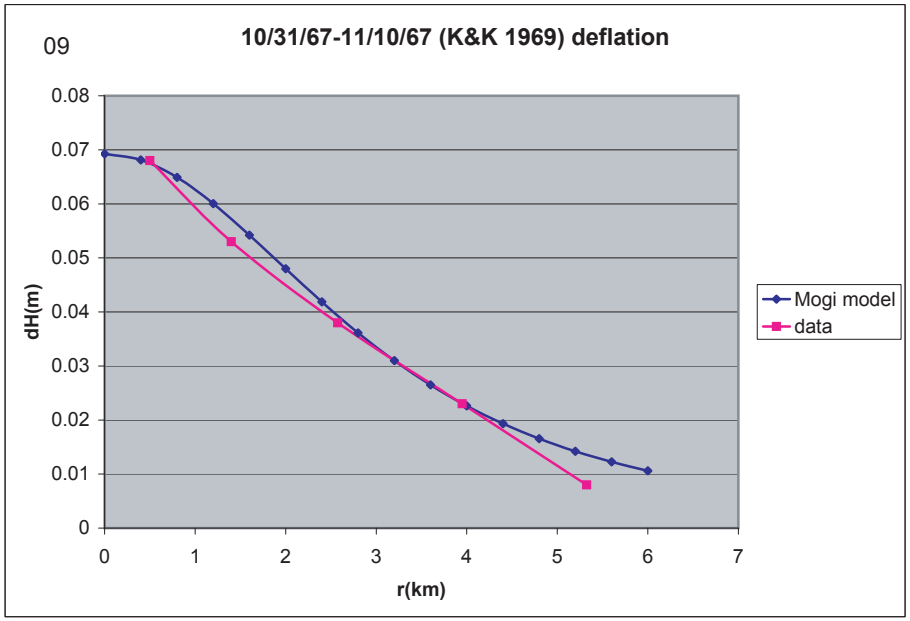

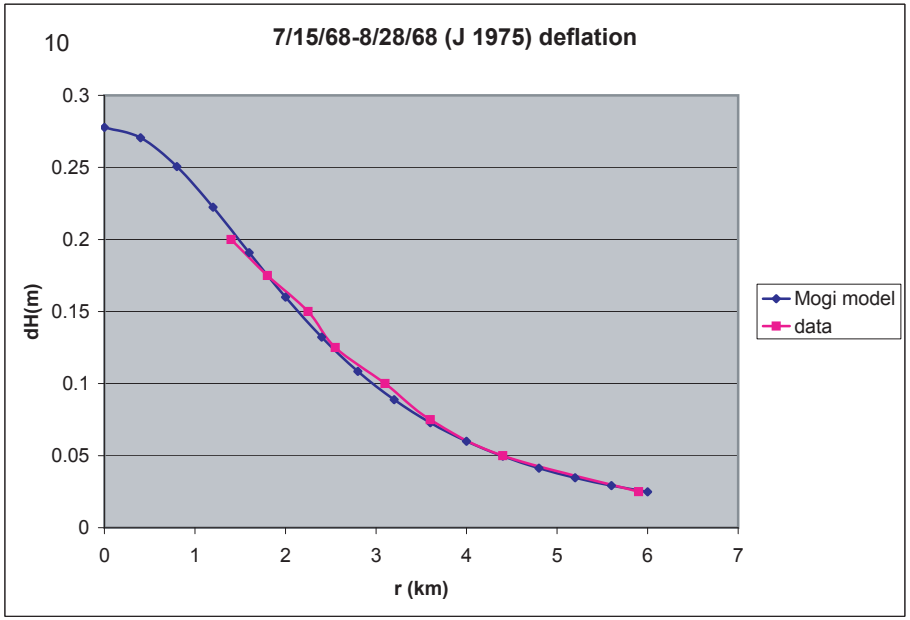

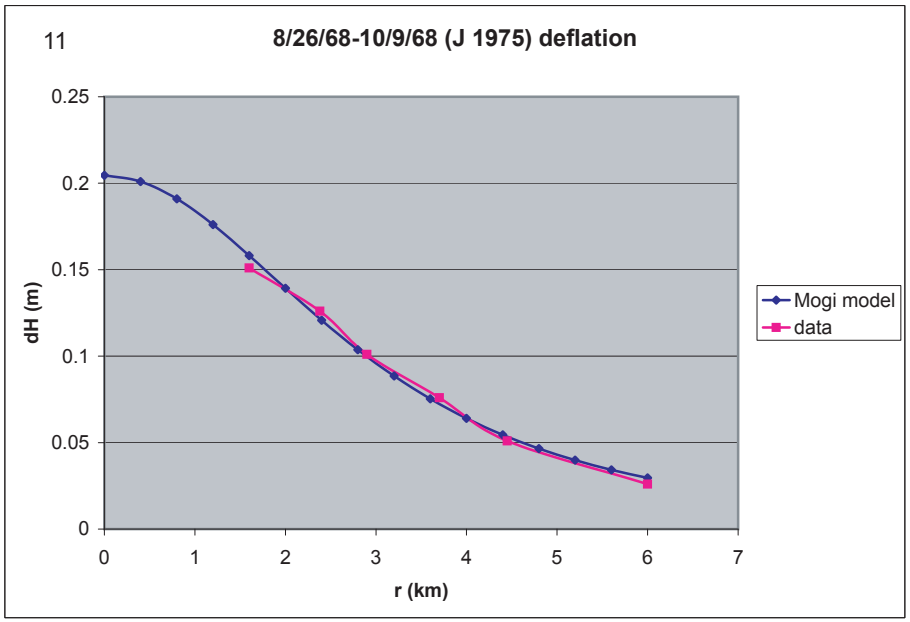

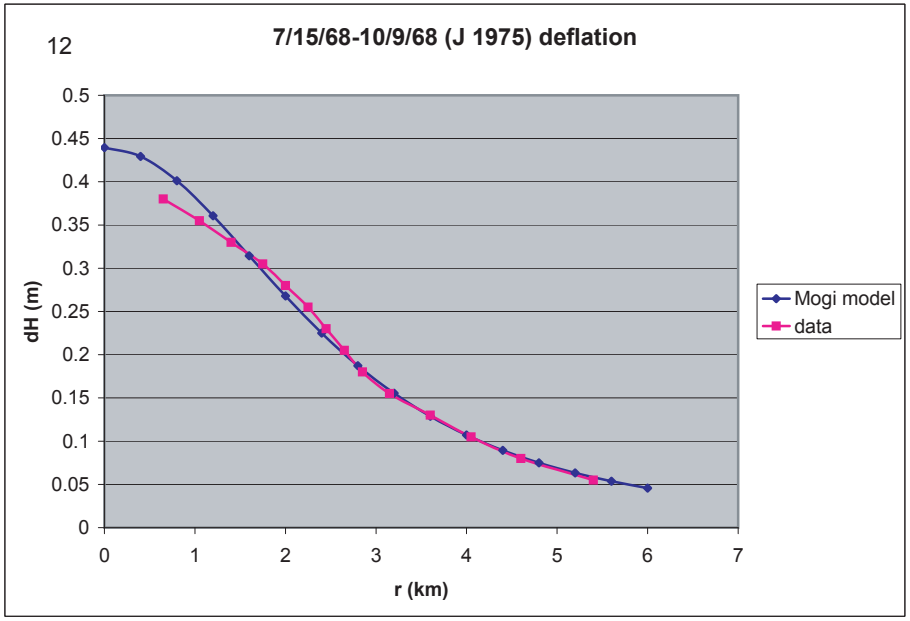

Appendix fig. I7.13-16. Mogi model fits to contoured levelling data. See table I1 for Mogi source data.

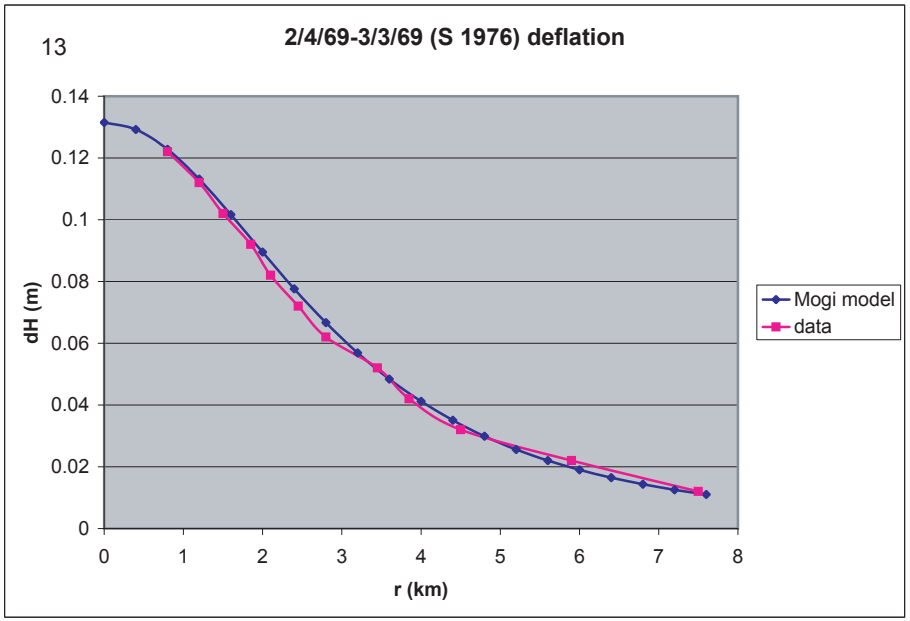

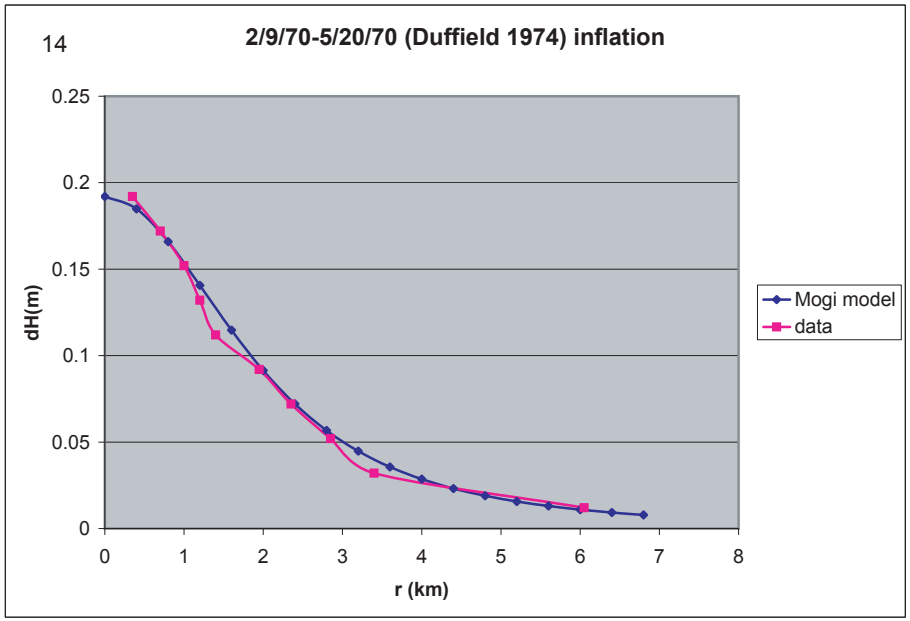

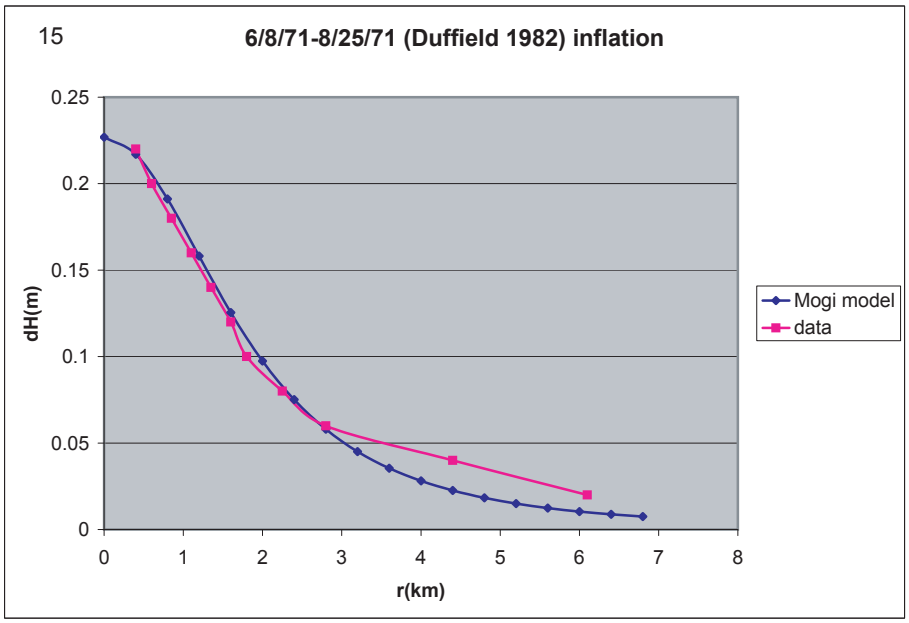

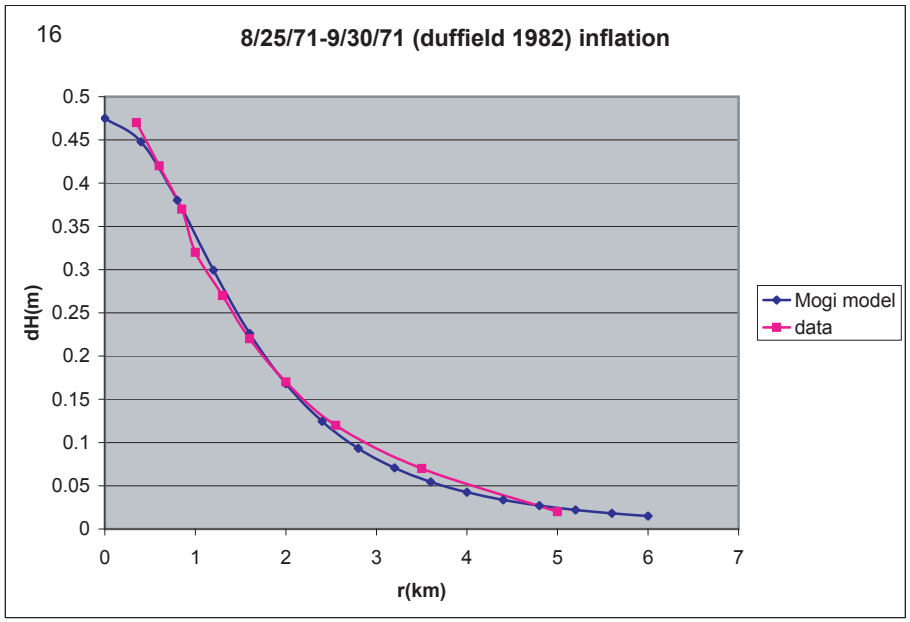

Appendix fig. I7.17-20. Mogi model fits to contoured levelling data. See table I1 for Mogi source data.

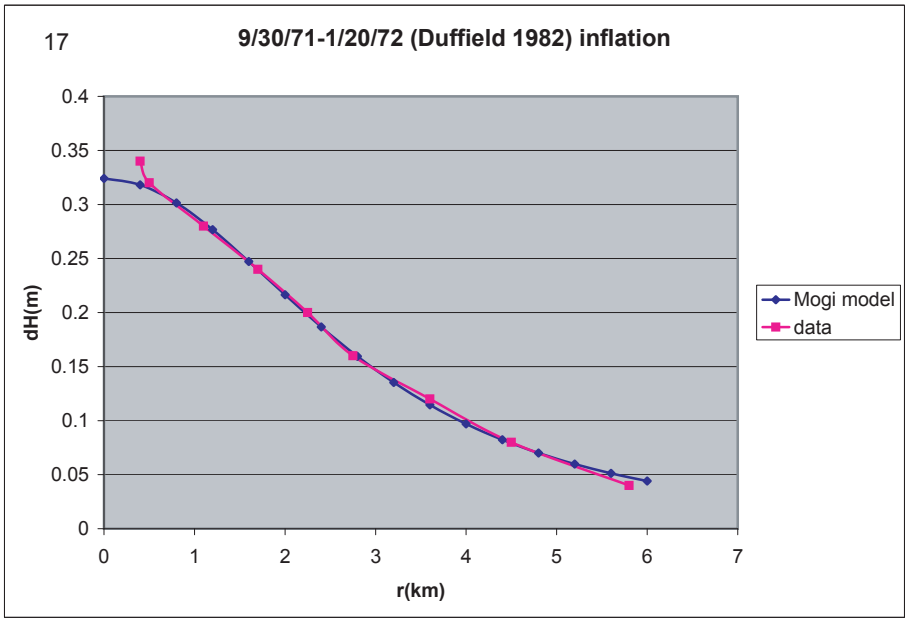

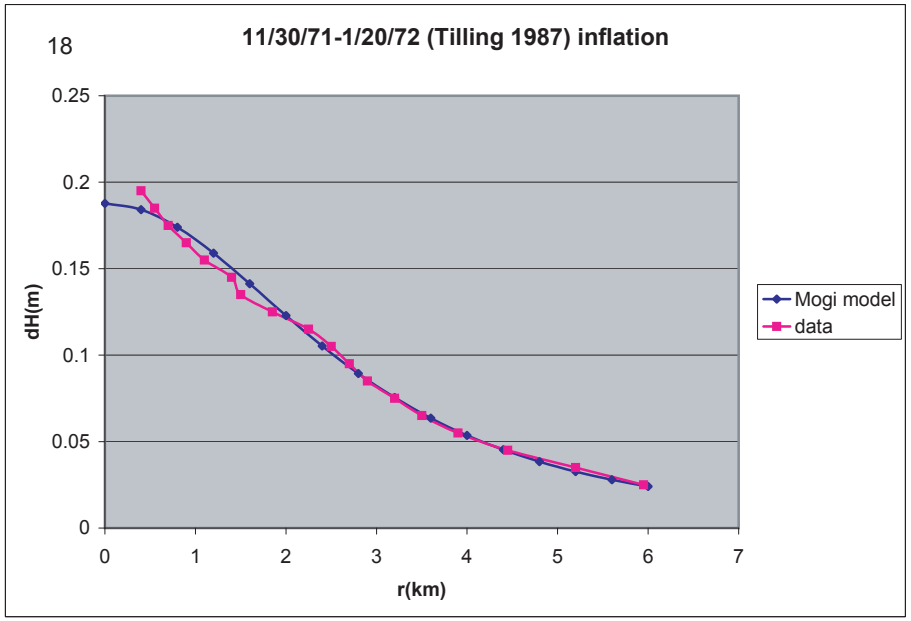

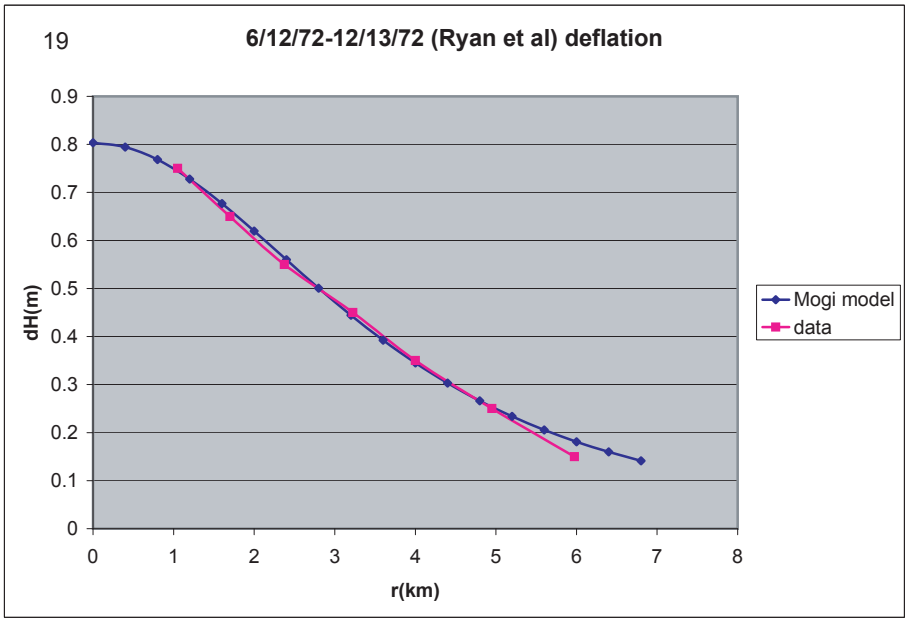

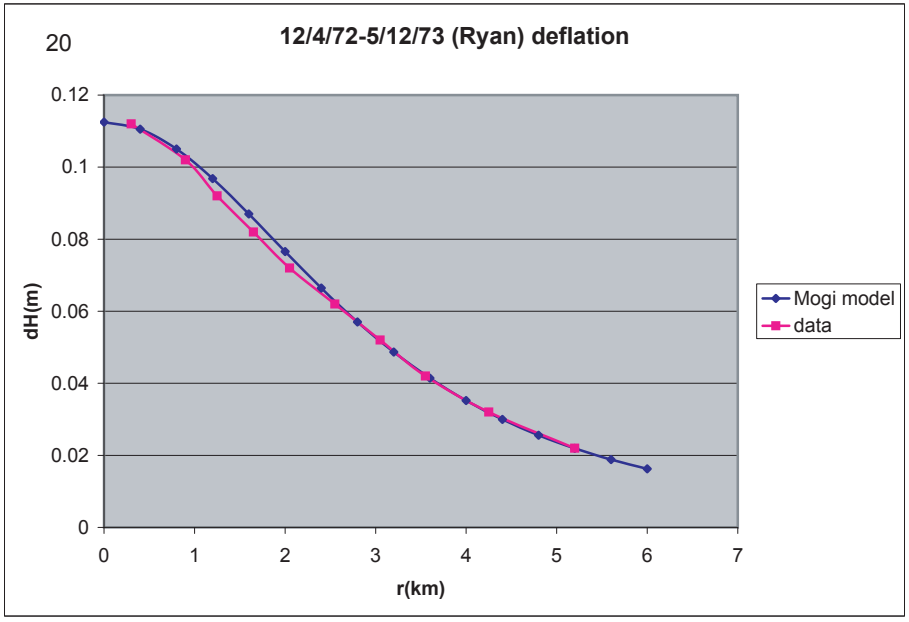

Appendix fig. I7.21-24. Mogi model fits to contoured levelling data. See table I1 for Mogi source data.

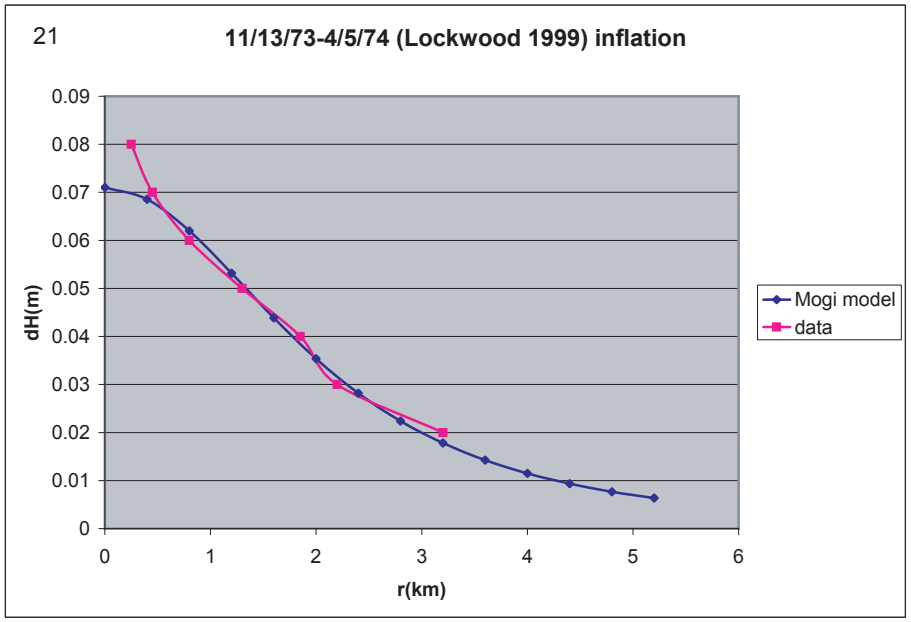

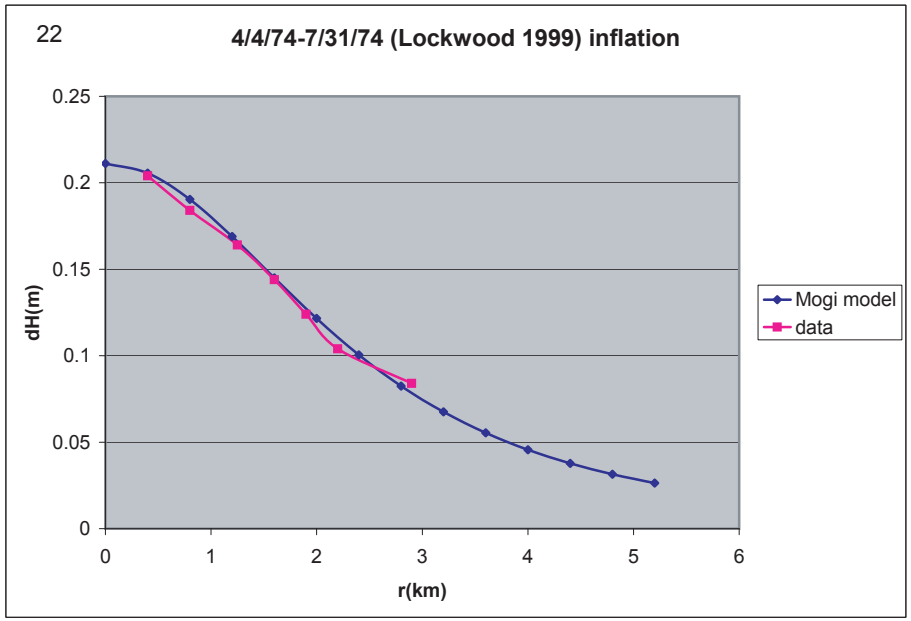

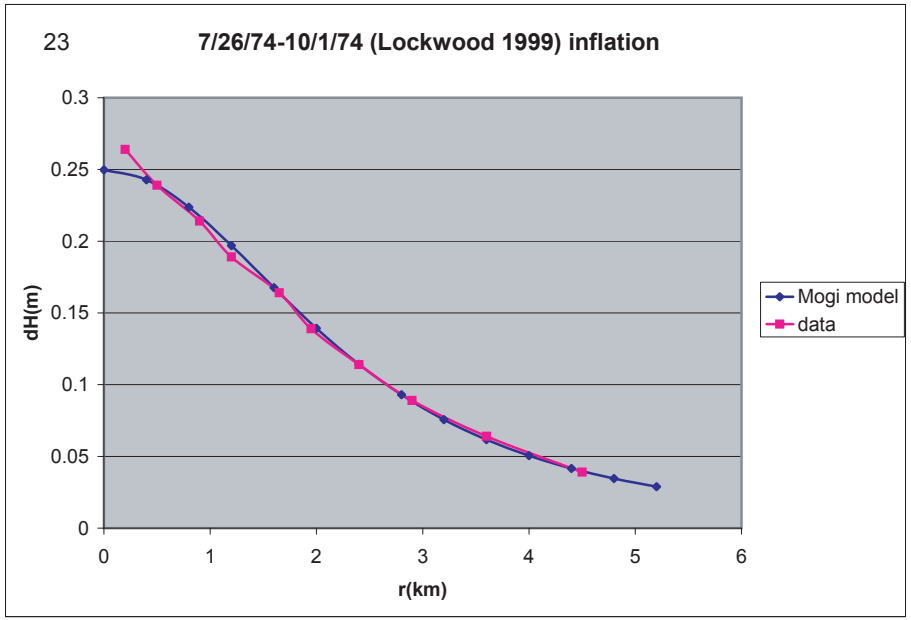

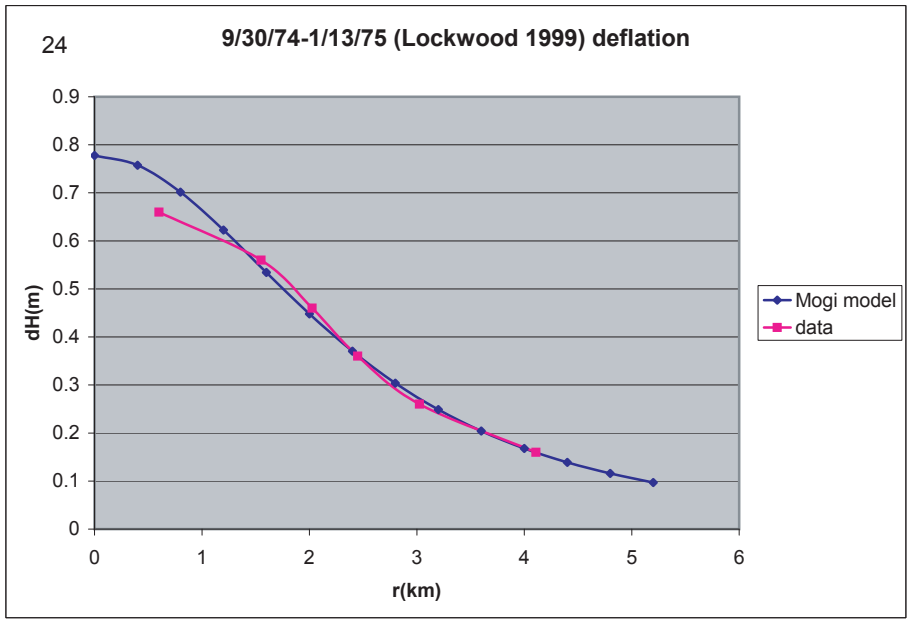

Appendix fig. I7.25-28. Mogi model fits to contoured levelling data. See table I1 for Mogi source data.

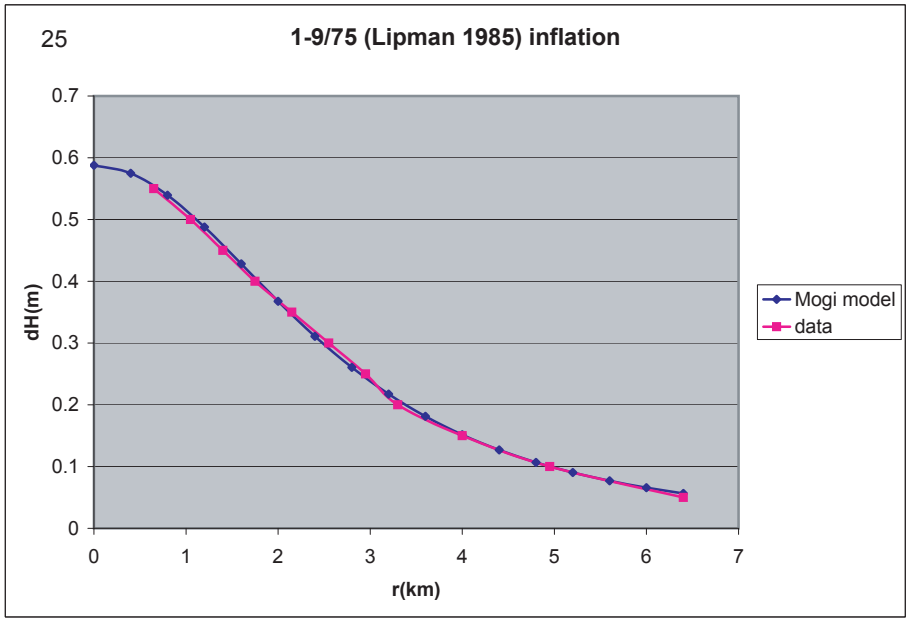

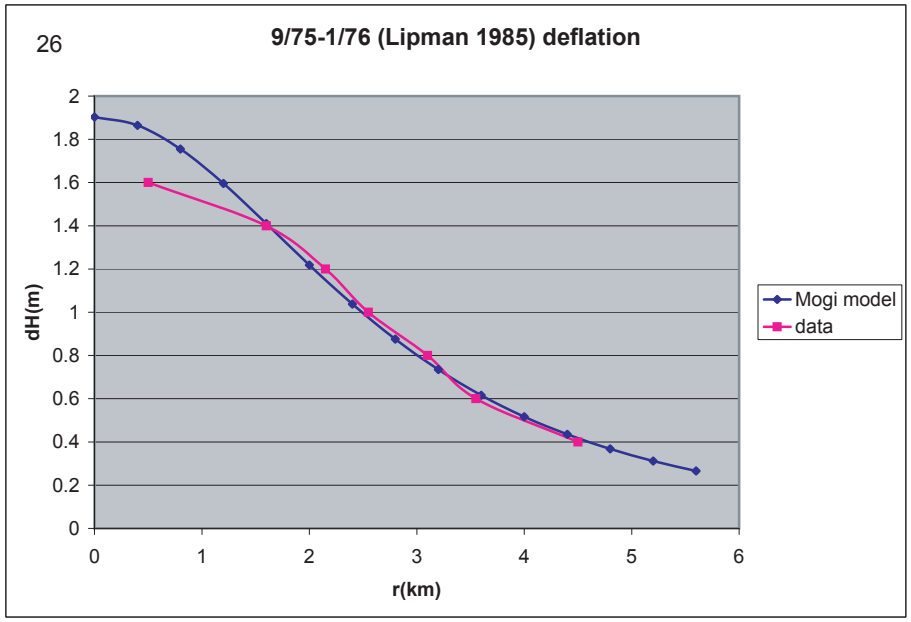

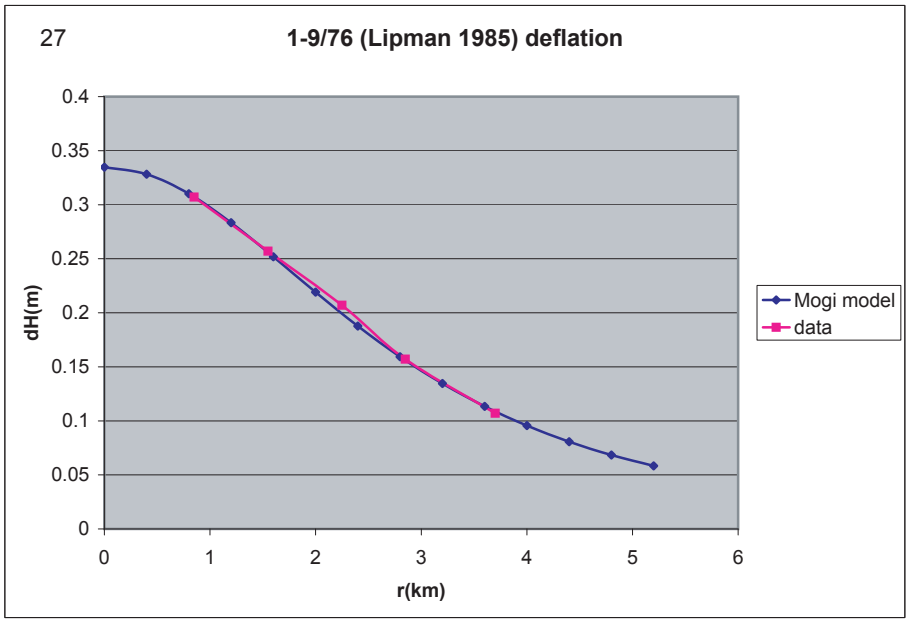

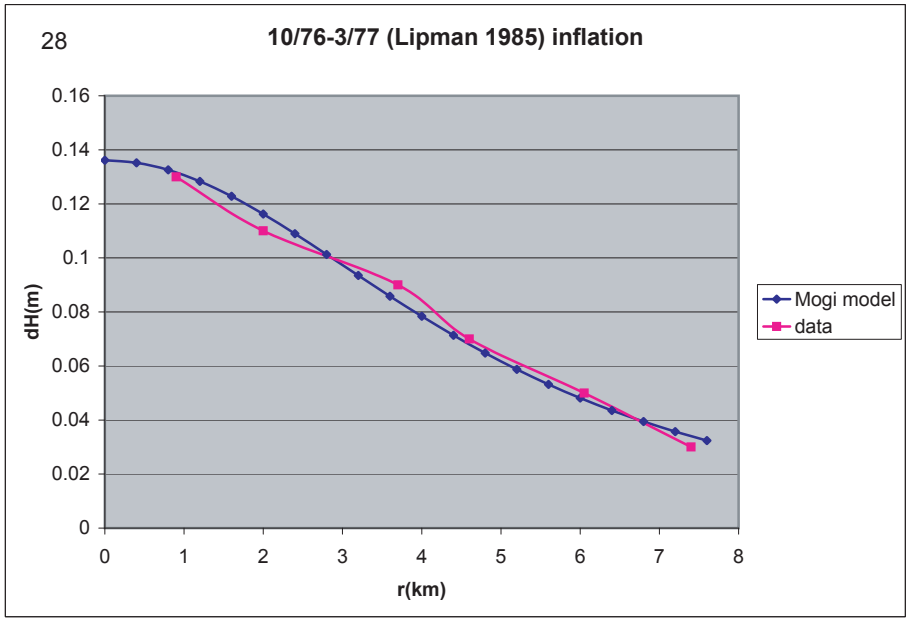

Appendix fig. I7.29-32. Mogi model fits to contoured levelling data. See table I1 for Mogi source data.

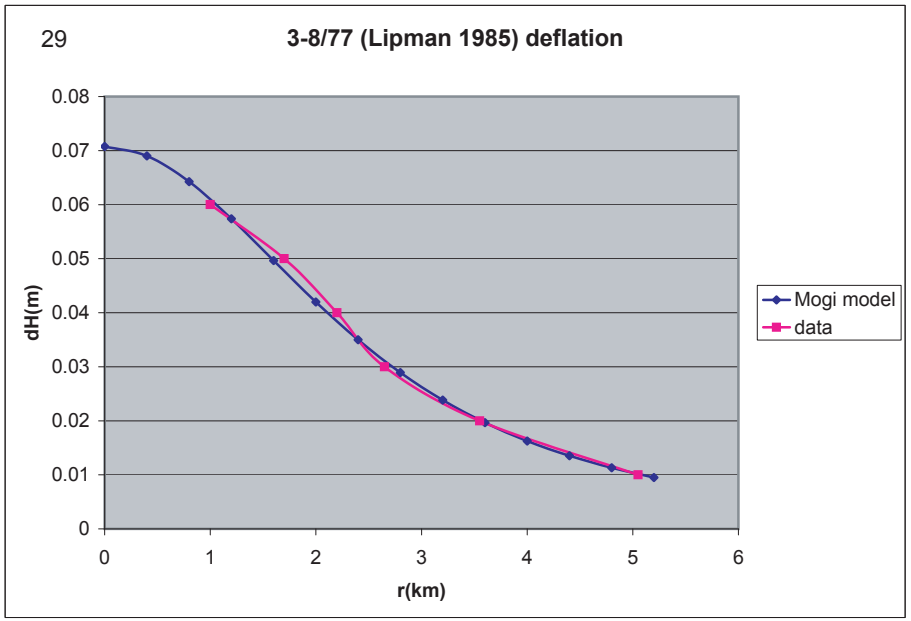

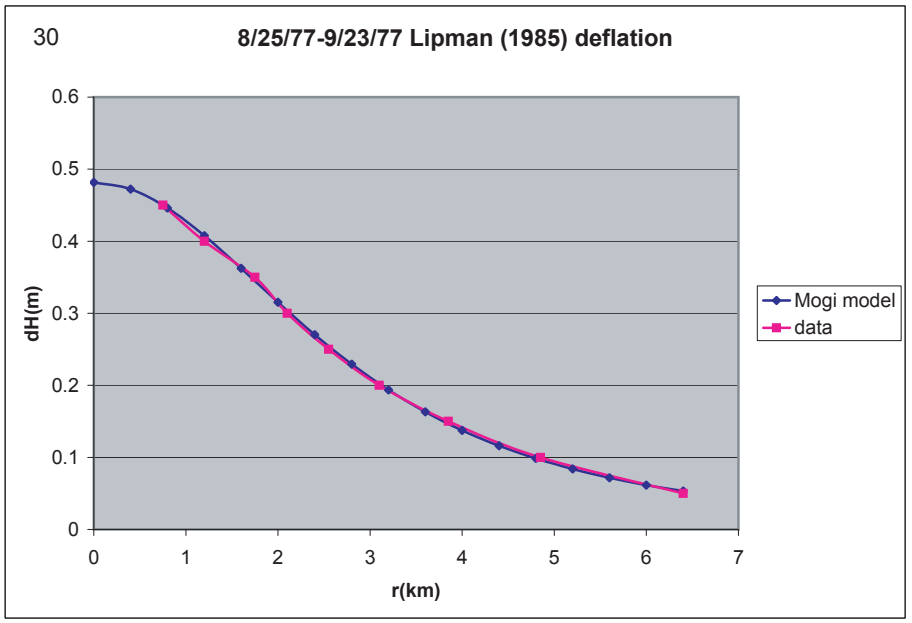

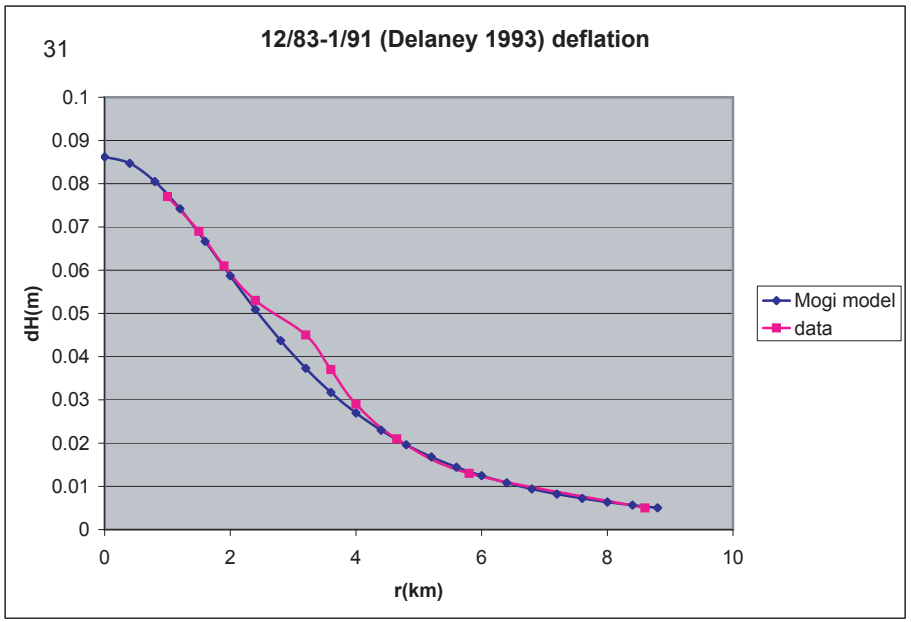

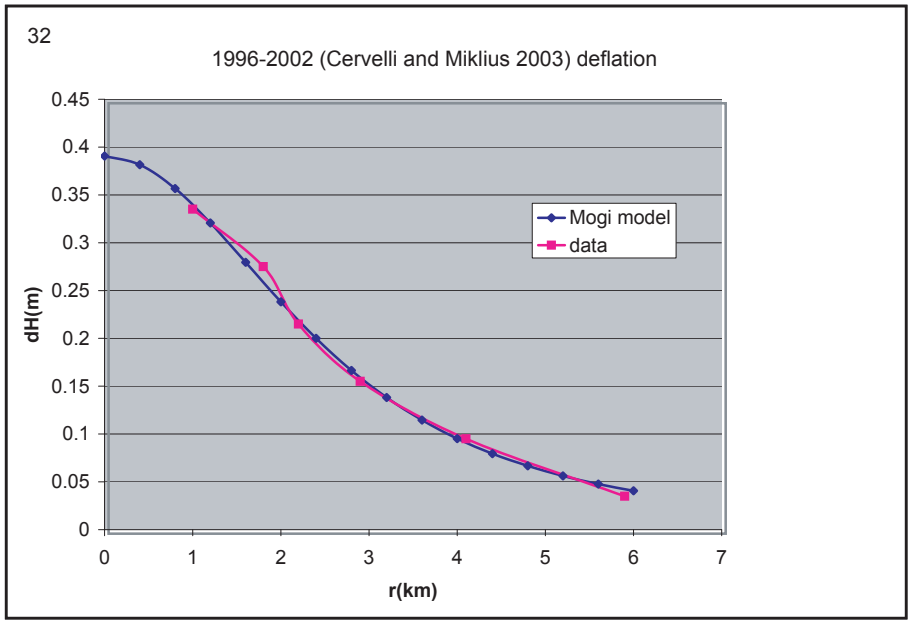

Appendix figure I8. Mogi volume changes vs. Mogi center depths for a set of level surveys.